RT NO. FRA/ORD-78/32,I

SELECTED TOPICS IN RAILROAD TANK CAR SAFETY RESEARCH
Volume I: Fatigue Evaluation of Prototype Tank Car Head Shield

Milton R. Johnson

IIT Research Institute
10 West 35th Street
Chicago IL 60616

AUGUST 1978

FINAL REPORT

Prepared for

U.S. DEPARTMENT OF TRANSPORTATION
FEDERAL RAILROAD ADMINISTRATION
Office of Research and Development
Washington DC 20590

NOTICE

This document is disseminated under the sponsorship of the Department of Transportation in the interest of information exchange. The United States Government assumes no liability for its contents or use thereof.

NOTICE

The United States Government does not endorse products or manufacturers. Trade or manufacturers' names appear herein solely because they are considered essential to the object of this report.

Technical Report Documentation Page

1. Report No	2. Government Accession No.	3. Recipient's Catalog No
FRA/ORD-78/32,I		

4. Title and Subtitle
SELECTED TOPICS IN RAILROAD TANK CAR SAFETY RESEARCH
Volume I: Fatigue Evaluation of Prototype Tank Car Head Shield

5. Report Date
August 1978

6. Performing Organization Code

7. Author's
Milton R. Johnson

8. Performing Organization Report No
DOT-TSC-FRA-78-12,I

9. Performing Organization Name and Address
IIT Research Institute*
10 West 35th Street
Chicago IL 60616

10. Work Unit No (TRAIS)
RR828/R8335

11. Contract or Grant No.
DOT-TSC-1043-1

12. Sponsoring Agency Name and Address
U.S. Department of Transportation
Federal Railroad Administration
Office of Research and Development
Washington DC 20590

13. Type of Report and Period Covered
Final Report
May 1975 to July 1976

14. Sponsoring Agency Code

15. Supplementary Notes
*Under contract to: U.S. Department of Transportation
Research and Special Programs Administration
Transportation Systems Center
Cambridge MA 08142

16. Abstract

The characteristics of a prototype head shield for hazardous material tank cars were evaluated with respect to the maintenance of its structural integrity under normal service conditions. The primary concern was with the resistance to fatigue damage of head shield connections to the tank car. The evaluation was conducted by performing tests on a tank car equipped with the shield. The shield and its supporting structure were instrumented to determine the principal forces acting within the structure and at points of attachment to the tank car. Both car-coupling impact and over-the-road tests were conducted. The impact tests were conducted at speeds of from 3 to 8 mph. The over-the-road tests included 432 miles of operation at speeds up to 55 mph. Evaluation of the data revealed that the car-coupling impact environment was the most severe. A finite fatigue life was indicated for the most severely stressed region of the supporting structure. The most severe over-the-road environment occurred with the loaded car at speeds above 45 mph when the main suspension bottomed out. The loads associated with this phenomenon were below those of the car-coupling impact environment.

This is the first volume of a two-volume report. Volume II, Test Plan for Accelerated Life Testing of Thermally Shielded Tank Cars, has 72 pages.

17. Key Words	18. Distribution Statement
Hazardous Material Tank Cars Tank Cars Head Shields Fatigue Analysis	DOCUMENT IS AVAILABLE TO THE U.S. PUBLIC THROUGH THE NATIONAL TECHNICAL INFORMATION SERVICE, SPRINGFIELD, VIRGINIA 22161

19. Security Classif. (of this report)	20. Security Classif. (of this page)	21. No. of Pages	22. Price
Unclassified	Unclassified	82	

Form DOT F 1700.7 (8-72) Reproduction of completed page authorized

METRIC CONVERSION FACTORS

Approximate Conversions to Metric Measures

Symbol	When You Know	Multiply by	To Find	Symbol
		LENGTH		
in	inches	2.5	centimeters	cm
ft	feet	30	centimeters	cm
yd	yards	0.9	meters	m
mi	miles	1.6	kilometers	km
		AREA		
in^2	square inches	6.5	square centimeters	cm^2
ft^2	square feet	0.09	square meters	m^2
yd^2	square yards	0.8	square meters	m^2
mi^2	square miles	2.5	square kilometers	km^2
	acres	0.4	hectares	ha
		MASS (weight)		
oz	ounces	28	grams	g
lb	pounds	0.45	kilograms	kg
	short tons (2000 lb)	0.9	tonnes	t
		VOLUME		
tsp	teaspoons	5	milliliters	ml
Tbsp	tablespoons	15	milliliters	ml
fl oz	fluid ounces	30	milliliters	ml
c	cups	0.24	liters	l
pt	pints	0.47	liters	l
qt	quarts	0.95	liters	l
gal	gallons	3.8	liters	l
ft^3	cubic feet	0.03	cubic meters	m^3
yd^3	cubic yards	0.76	cubic meters	m^3
		TEMPERATURE (exact)		
°F	Fahrenheit temperature	5/9 (after subtracting 32)	Celsius temperature	°C

Approximate Conversions from Metric Measures

Symbol	When You Know	Multiply by	To Find	Symbol
		LENGTH		
mm	millimeters	0.04	inches	in
cm	centimeters	0.4	inches	in
m	meters	3.3	feet	ft
m	meters	1.1	yards	yd
km	kilometers	0.6	miles	mi
		AREA		
cm^2	square centimeters	0.16	square inches	in^2
m^2	square meters	1.2	square yards	yd^2
km^2	square kilometers	0.4	square miles	mi^2
ha	hectares (10,000 m^2)	2.5	acres	
		MASS (weight)		
g	grams	0.035	ounces	oz
kg	kilograms	2.2	pounds	lb
t	tonnes (1000 kg)	1.1	short tons	
		VOLUME		
ml	milliliters	0.03	fluid ounces	fl oz
l	liters	2.1	pints	pt
l	liters	1.06	quarts	qt
l	liters	0.26	gallons	gal
m^3	cubic meters	35	cubic feet	ft^3
m^3	cubic meters	1.3	cubic yards	yd^3
		TEMPERATURE (exact)		
°C	Celsius temperature	9/5 (then add 32)	Fahrenheit temperature	°F

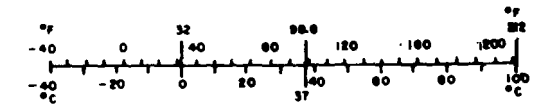

PREFACE

The work described in this report was conducted by IIT Research Institute (IITRI) under the authorization of Transportation Systems Center (TSC) Contract DOT-TSC-1043. The report is issued in two volumes. Volume I describes the evaluation of the structural integrity of a prototype tank car head shield when exposed to conditions representative of the normal service environment. Volume II describes a test plan for accelerated life testing of thermally shielded tank cars.

The prototype head shield was designed by Louisiana Tech University, under the direction of Dr. Mike Wilkinson. The design of the shield was a modified version of a similar shield which had been tested earlier.

The car-coupling impact tests were carried out at the Research and Development Division of Miner Enterprises Inc., Chicago, Illinois under the direction of Mr. Robert Arseneau. The over-the-road tests were conducted through cooperation with the Illinois Central Gulf Railroad. The shield was installed on a car provided through arrangements with the Railway Progress Institute/Association of American Railroads (RPI/AAR) Tank Car Safety Project. The instrumented side bearings used on the over-the-road tests were provided through Mr. R. Evans, Project Director, RPI/AAR Truck Research Safety and Test Project.

Dr. M. R. Johnson was IITRI project manager for this work. Other staff members who contributed to this project include Mr. E. Scharres and Mr. Glenn Kutzer of the Experimental Operations Section who directed data recording activities. Mr. G. Ebey assisted in the analysis of the data, and Mr. P. Cannon of the Digital Systems Group processed that portion of the data requiring computer analysis. Dr. A. Robert Raab was the cognizant TSC Technical Monitor. His helpful suggestions and guidance throughout the course of the work are gratefully acknowledged.

TABLE OF CONTENTS

LIST OF ILLUSTRATIONS

LIST OF ILLUSTRATIONS (Concl)

LIST OF TABLES

EXECUTIVE SUMMARY

The characteristics of a prototype head shield for hazardous material tank cars were evaluated with respect to the maintenance of its structural integrity under normal service conditions. The primary concern was with the resistance to fatigue damage of head shield connections to the tank car. The evaluation of the shield's ability to reduce the probability of head puncture in the accident environment was not within the scope of this program.

Head shields are applied to tank cars for protection against puncture. The principal hazard occurs in derailments or under high-speed car-coupling impacts. Under these conditions if cars separate the couplers of adjacent cars may be forced against the tank heads causing their rupture and the subsequent release of hazardous materials. The addition of a head shield at the ends of cars is expected to be an effective means of reducing such punctures.

To retain their effectiveness the shields must remain fixed securely to the cars throughout their expected lifetimes. Fatigue damage of the tank shell or of the structural components of the car to which the shield is attached, may develop during normal service operations resulting in damage to the basic car structure or the shield. If significant fatigue damage should occur there is the possibility of separation of the shield from the car.

The prototype head shield evaluated in this program was designed and fabricated by Louisiana Tech University. The evaluation was conducted by performing tests on a tank car equipped with the shield. The shield and its supporting structure were instrumented to determine the principal forces acting within the structure and at points of attachment to the tank car. Both car-coupling impact and over-the-road tests were conducted. Forty-one impact tests were conducted at speeds of from 3 to 8 mph. The over-the-road tests included 432 miles of operation at speeds up to 55 mph.

Three different versions of the side supporting structure for the shield were included in the tests. The differences were in the flexibility of the side supports which connect the shield plate to the car bolster. As expected the shield with the most flexible side supports deflected most in response to the inertial loads associated with car impacts. For each design version the most severely stressed element was the horizontal support angle. This member spans between the two side sills and the stub sill and supports the weight of the shield. Within this element the highest stresses were developed at its junction with the stub sill. The stresses in this member were slightly lower with the more rigid side supports than with the flexible side supports.

The data obtained from transducers mounted on the structure were analyzed to determine the fatigue characteristics of the design. The analysis showed that car-coupling impacts produced an environment where finite life would be expected at the most highly stressed location in the supporting structure. The over-the-road operations revealed a less severe environment where fatigue damage would not be anticipated. The evaluation was based on the reported number of car coupling impacts that an average car would experience yearly and the velocity distribution of these impacts. A relatively small design change in the support structure for the shield would be sufficient to eliminate any possibility of fatigue damage.

The forces transmitted to the car body itself from the shield were determined for both the car-coupling impact and over-the-road environments. These forces are transmitted through the side supports to the car bolster and through the horizontal supporting member to the side sills and stub sill. They were found to be of negligible magnitude on the over-the-road environment. The forces transmitted to the car during car-coupling impacts were significantly larger, but were still within the limits where they could be reacted by the existing car structure without causing damage. Thus the addition of the head shield to a hazardous material tank car is possible without altering the structural configuration of the end of the car.

There are two basic factors which should be recognized when considering head shield qualification tests:

The fact that the car-coupling environment produces more significant effects on the shield and supporting structure than the over-the-road environment and,

the fact that tests are necessary to demonstrate the shield performance because of the complex response of the shield to the dynamic service environment (whether it be car-coupling impacts or over-the-road).

Qualification tests are required because of the complex dynamic response of the head shield and its supporting structure to the car-coupling impact environment. In the tests it was noted that the response of higher-order vibrational modes gave significant contributions to the damage producing phenomena. These response phenomena will not be revealed by simplified analyses which account for only the fundamental vibrations of the shield structure. A complex structural analysis with an accurate dynamic representation of all structural characteristics would be required to predict motions and magnitudes of the loads like those which were measured. By testing in the actual physical environment the response parameters can be measured which have to be considered in the evaluation of the fatigue characteristics.

While the qualification test can be limited to car-coupling impact tests, one should recognize the strong dependence of the test results on the specific conditions under which the test is conducted. In this study, for example, the rate of accumulation of fatigue damage with the anvil car tests was eight times greater than with the hammer car tests. The reason for this difference is the fact that the higher modal frequencies of the shield supporting structure are significant in affecting maximum loads and stresses within the structure. Slight differences in properties of the acceleration phenomena associated with the placement of the shield on the test car and the condition of restraint and deceleration of the cars themselves, has an important effect in determining maximum stresses and strains within the structure. Therefore one should consider conducting several types of car-coupling impact tests in any head shield qualification procedure so that the most significant dynamic phenomena will be identified in the testing process.

1. INTRODUCTION

1.1 Objective

An evaluation of a prototype head shield for hazardous material tank cars with respect to the maintenance of its structural integrity under normal service conditions was performed. The principal objective of this study was to determine if the head shield connections to the tank car would resist fatigue damage under both car-coupling impact and over-the-road environments. The evaluation of the shield ability to reduce the probability of head puncture in the accident environment was not within the scope of this program.

1.2 Background

This project was part of a larger Federal Railroad Administration (FRA), Transportation Systems Center (TSC) program dealing with the application of tank car head shields for protection against puncture. The concern is with cars carrying hazardous liquified gases under pressure. The principal hazard occurs in derailments or under high-speed car coupling impacts. Under these conditions if cars separate the couplers of adjacent cars may be forced against the tank heads causing their rupture and the subsequent release of hazardous materials. The addition of a head shield at the ends of cars is expected to be an effective means of reducing such punctures.

To retain their effectiveness the shields must remain fixed securely to the cars throughout their expected lifetimes. Fatigue damage of the tank shell or of the structural components of the car to which the shield is attached, may develop during normal service operations resulting in damage to the basic car structure or the shield. If significant fatigue damage should occur there is the possibility of separation of the shield from the car.

Under FRA authorization, Louisiana Tech University (LTU) designed and fabricated a prototype head shield. The specific configuration of the shield was slightly modified from a design which had been evaluated earlier (Ref. 1) under car-coupling impact conditions. Three different designs of side supporting structures for the shield plate were used during the car-coupling impact tests conducted as part of this evaluation.

The evaluation of the head shield involved three general tasks:

- definition of the loads acting between the shield and tank car under various service conditions,
- determination of the fatigue damage sensitivity of the prototype head shield design including the calculation of service life expectancy,
- establishment of guidelines for securing high-integrity long-life attachment of head shields to tank cars.

1.3 Characteristics of LTU Shield

The principles which are followed in the LTU shield design are to avoid direct attachment to the tank head and minimize load transfer to the stub sill. The weight of the shield is supported by a structural member which spans the width of the car between the side sills. This member also rests on the stub sill, which therefore supports some of the weight of the shield. The upper portion of the shield is held in position by two members, one on each side of the car, which connect the sides of the shield with the tank car bolster. Two different designs of this member have been tested, one providing more flexibility than the other in the longitudinal direction. The head shield configuration and the nomenclature used in this report are given in Figure 1.

Figure 2 shows the version of the shield which utilizes a strap side support between the shield and the tank car bolster. The strap provides substantial flexibility in the longitudinal direction. Figure 3 shows the version of the shield which utilizes a tube support member between the shield and the tank car bolster.

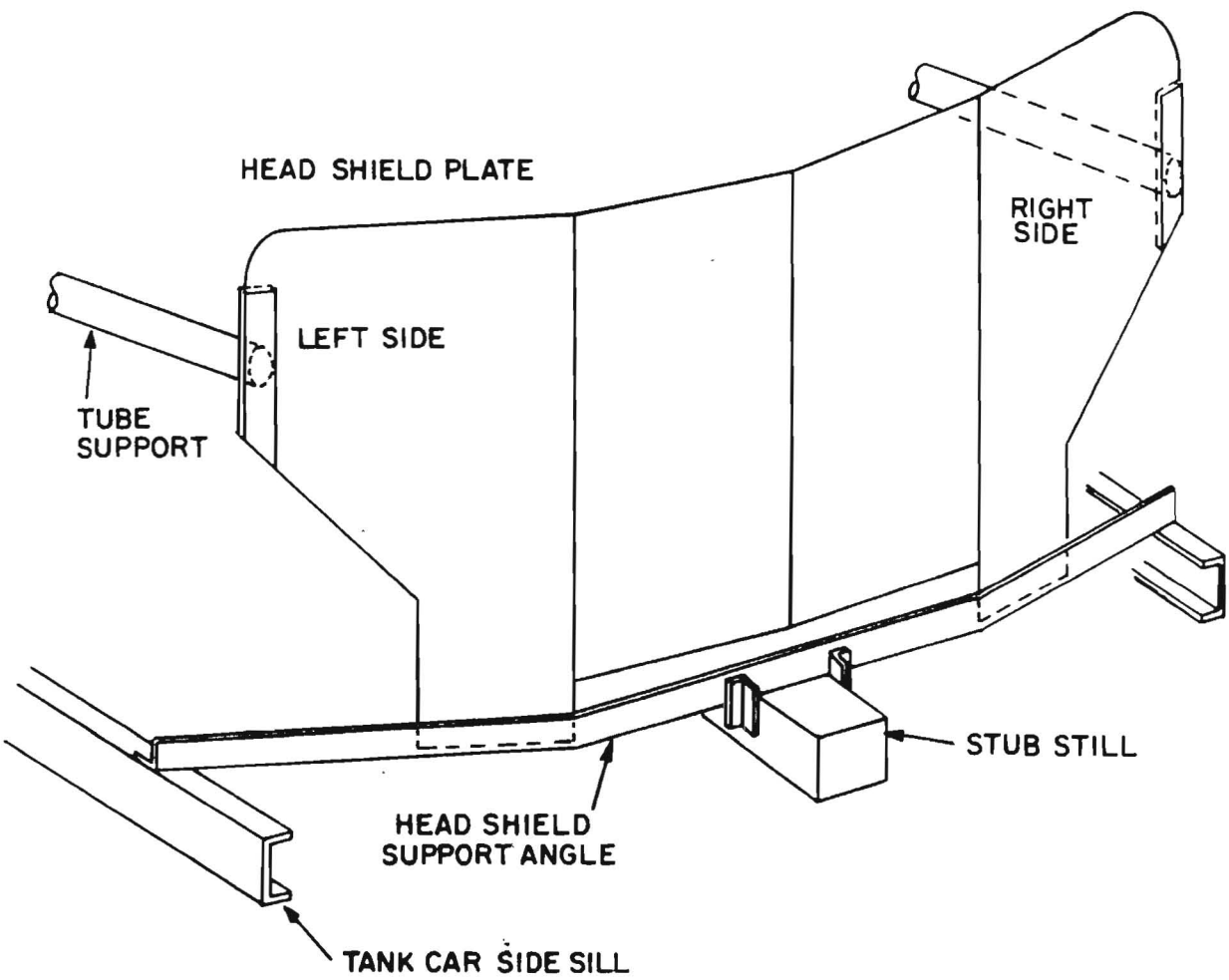

FIGURE 1. HEAD SHIELD CONFIGURATION NOMENCLATURE.

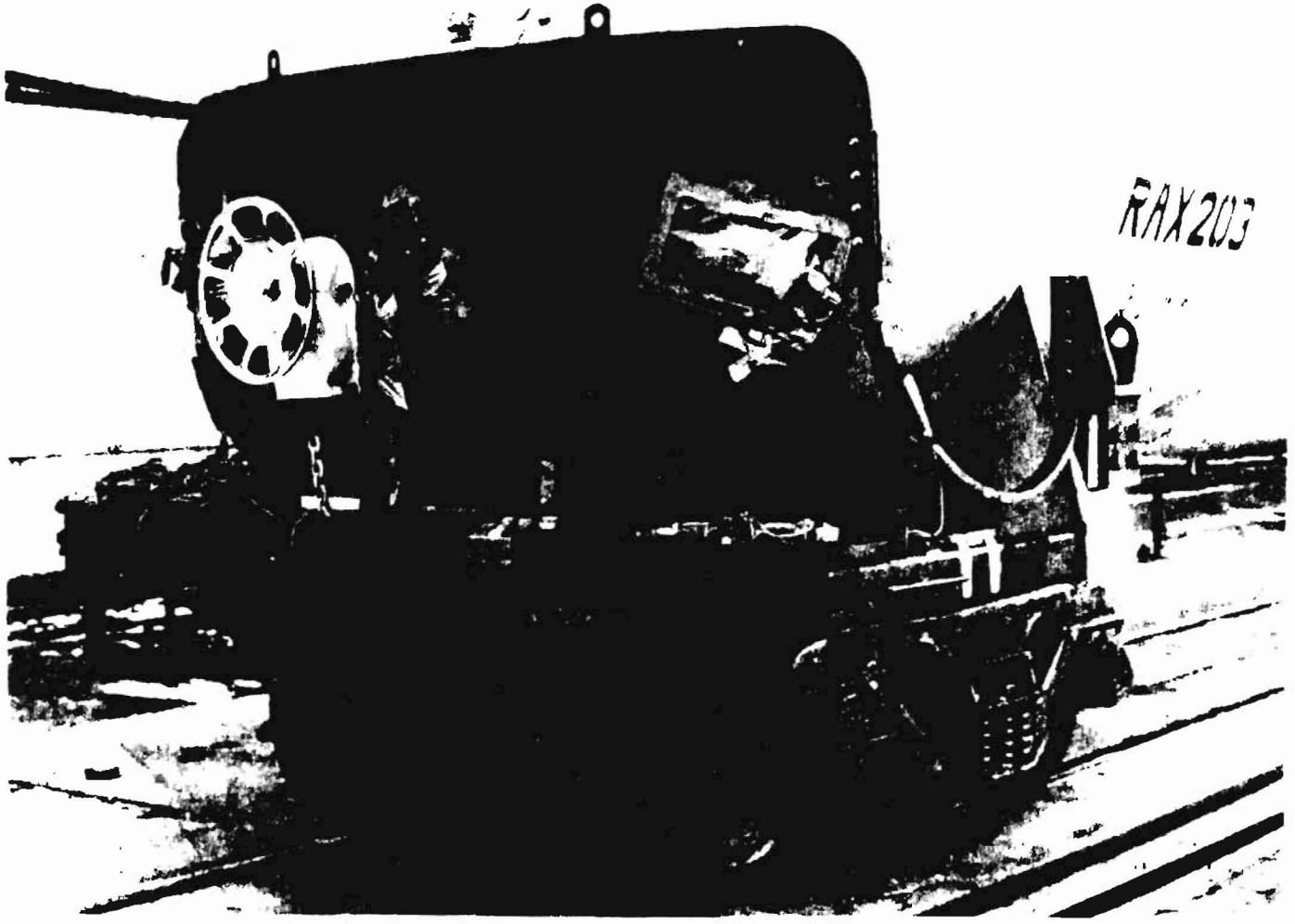

FIGURE 2. SHIELD WITH STRAP SIDE SUPPORT CONNECTION TO BOLSTER.

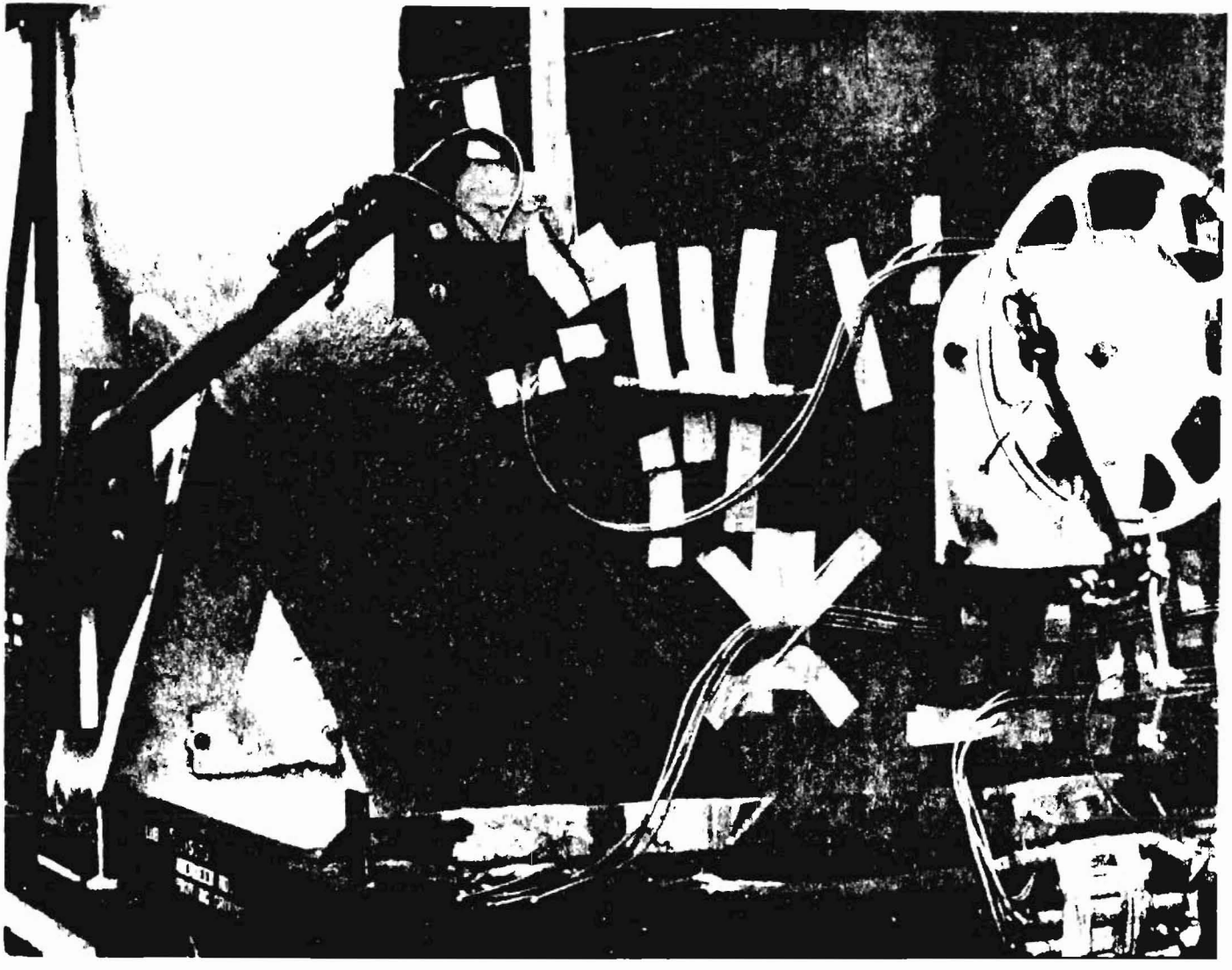

FIGURE 3. SHIELD WITH TUBE SIDE SUPPORT CONNECTION TO BOLSTER.

This design provides a more rigid connection in the longitudinal direction. A detailed view of the horizontal supporting angle is shown in Figure 4. This figure illustrates the support given by the stub sill to this angle at the center of the car. In an earlier version of the shield the angle only rested on the stub sill and was not directly connected to it. This lead to excessive vertical vibrations. The angle was subsequently welded to the stub sill. The data presented in this report deal exclusively with the latter version of the shield supporting structure.

Some car-coupling impact tests were conducted with a special version of the flexible strap support. This included the use of a shock absorber between the points of connection of the flexible strap as illustrated in Figure 5. The over-the-road tests were conducted with only the use of the rigid tube side supports.

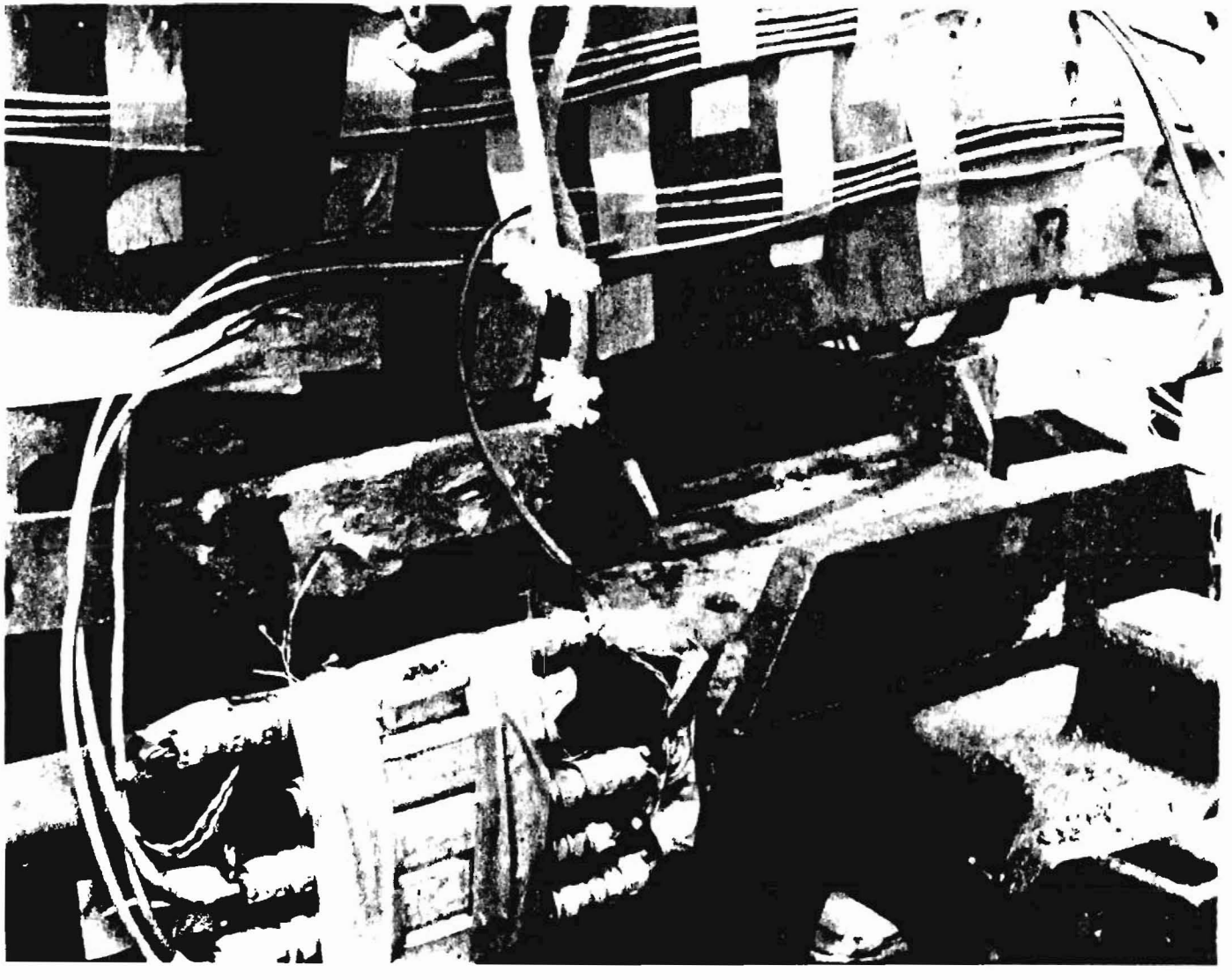

FIGURE 4. DETAIL OF SUPPORT ANGLE CONNECTION TO STUB SILL.

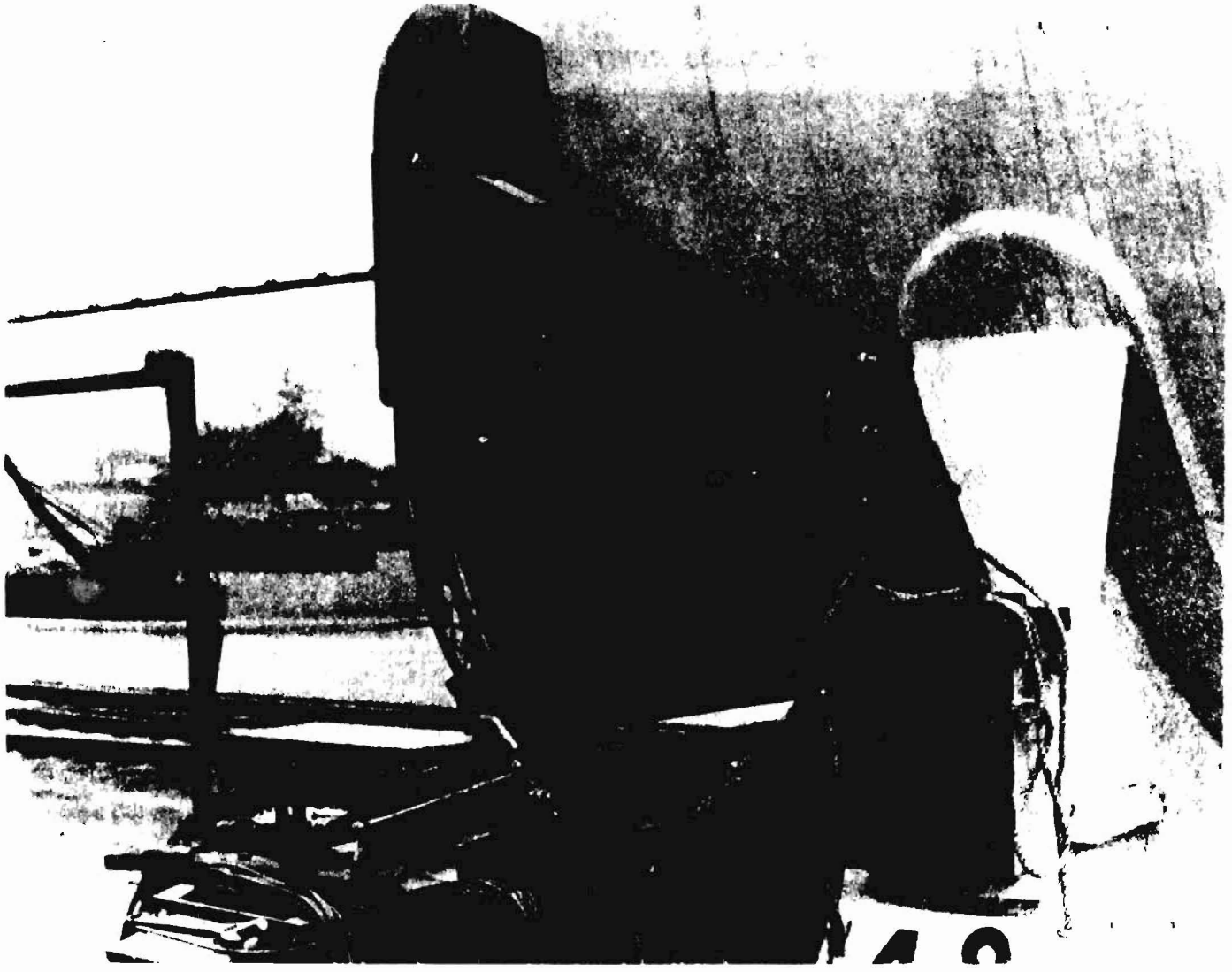

FIGURE 5. ARRANGEMENT OF SHOCK ABSORBER USED WITH STRAP SIDE SUPPORT.

2. TEST PLAN - CAR COUPLING IMPACTS

A review of the head shield design indicated that the most severe load environment probably would be the inertial loads accompanying sudden accelerations of the car. It was decided that the behavior of the shield under car-coupling impact conditions would be the first aspect of the load environment to be evaluated.

2.1 Test Procedures

The prototype head shield was installed on a 33,000 gallon capacity tank car built in conformance to DOT specification 112A340W for noninsulated pressure tank cars. The car, designated RAX 203, had an empty weight of 91,200 lb and an allowable loaded rail load of 263,000 lb. It was equipped with a draft gear conforming to AAR specification M-901E. The shield and tank car were instrumented with transducers to provide a continuous output of strains on the support angle, side supports and shield, displacement of shield, and coupler force. The shield was installed on the B-end (hand brake end) of the car.

Three types of impact tests were conducted. The first test was in accordance with paragraph 24-5 of the AAR Tank Car Specifications (Ref. 2). This test is specified as a method of evaluating head shields on hazardous material tank cars. The test is conducted by impacting a loaded car into a standing tank car equipped with the head shield. The shield is on the struck end of the car as illustrated in Figure 6a. The tank car, loaded with water to a rail load of 263,000 lb, was backed up by two standing hopper cars, each loaded to a 220,000 lb rail load. In addition, the hand brakes of the standing cars were applied and track skates were placed behind one set of wheels on each car.

The striking or hammer car was accelerated to predetermined velocities by releasing it on an inclined ramp. The first impact test was conducted at approximately 3 mph and subsequent impact velocities were increased in approximately 1 mph increments.

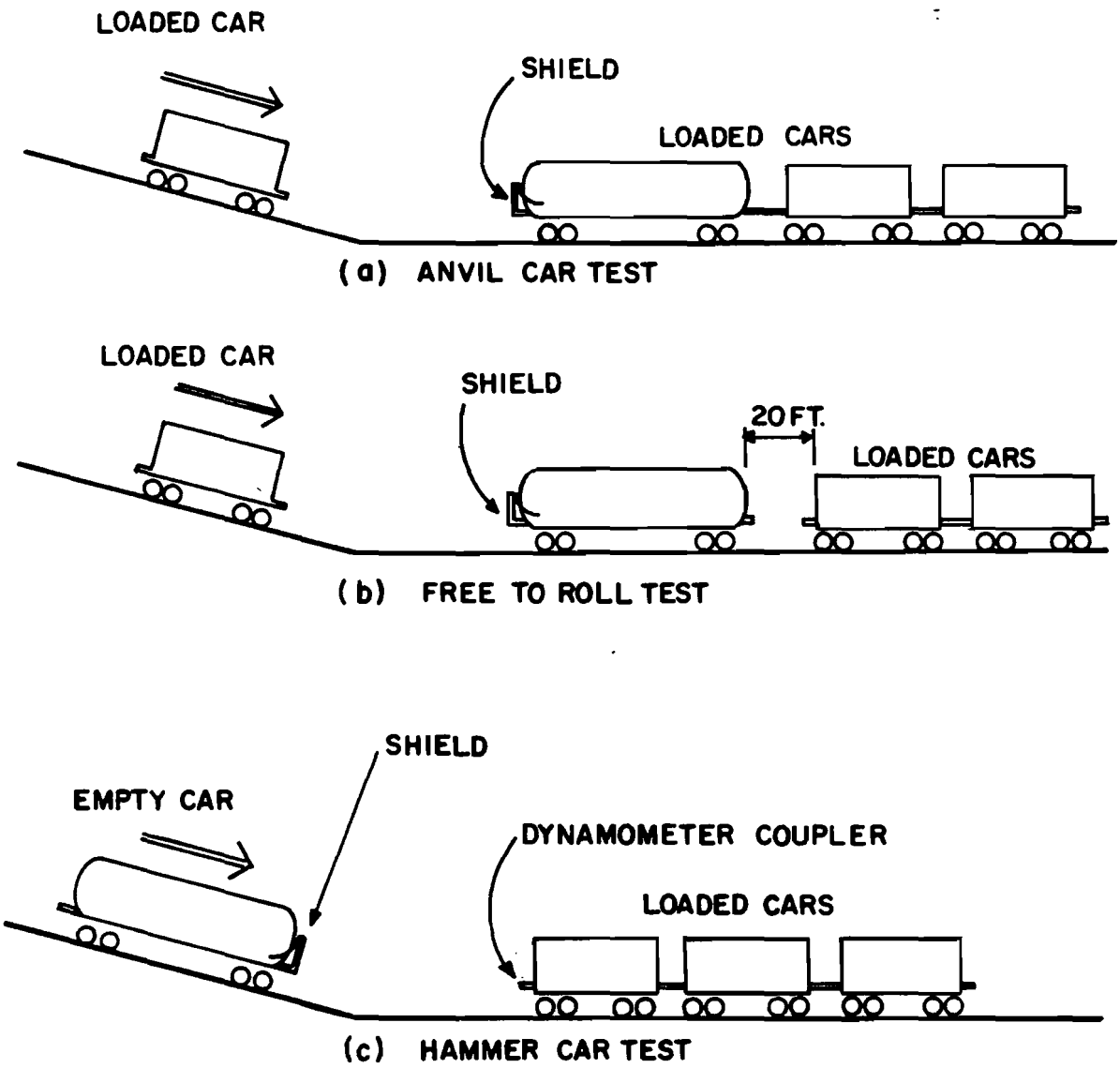

FIGURE 6. ARRANGEMENT OF CARS FOR IMPACT TESTS.

The impact velocities were increased until the force limitation (approximately 1,200,000 lb) was reached in the dynamometer coupler. This test procedure is subsequently referred to as the "anvil car" test.

The second test was the "free to roll" test. This test consisted of impacting a loaded car into the free standing, unloaded, tank car (free to roll) equipped with the head shield as illustrated in Figure 6b. This test differs from the anvil car test in that the tank car was allowed to roll approximately 20 ft before contacting the two backup hopper cars. The tank car was unloaded for this test.

The third test was the "hammer car" test. The unloaded tank car was impacted into three standing hopper cars, each loaded to a 220,000 lb rail load. The car was positioned so that the head shield was on the leading (striking) end of the car as shown in Figure 6c. Under these conditions the primary load acting on the shield is a longitudinal inertial load which results from the sudden deceleration of the car when it is stopped by impacting into the standing cars. The three standing cars were equipped with draft gear conforming to AAR specification M-901. The hand brakes of the standing cars were applied and track skates were placed behind one set of wheels on each car. It was recognized that this resulted in more severe resisting forces to the impacting tank car than free standing cars, but the test setup represented an upper limit to the severity of the conditions that can be found in service and allowed close control in the repeatability of test conditions. The tank car was empty for the hammer car tests since this would result in more severe decelerations than tests with a loaded car.

In all, six series of impact tests were conducted. The tests conducted with each version of shield side support are indicated as follows:

Design Version	Anvil Car Test	Anvil Car Free to Roll Test	Hammer Car Test
Strap Side Supports	x		x
Strap Side Supports with Shock Absorbers			x
Tube Side Supports	x	x	x

2.2 Instrumentation

The instrumentation was used to monitor the magnitude of the forces transmitted to the car from the shield through the points of shield interconnection with the car structure, the vibrational response of the shield to the impact, and strain levels within the shield. Transducers used to develop the data are listed in Table 1 and described in subsequent paragraphs. The locations of the transducers are shown in Figure 7 through 11.

Strain gages (Figure 7) were used to determine the stress field in the plate adjacent to the side support connections. The data from these gages were also used to identify principal vibrational frequencies. Additional strain gages, oriented horizontally, were placed on the front and back side of the plate near the center (Figure 7).

Strain gages (Figure 8) mounted on the side supports were used to determine the longitudinal inertial loads transmitted to the car structure through these elements. When the strap side supports were used, strain gages wired into bending bridges were placed at two elevations as shown in Figure 8. The magnitude and elevation of the longitudinal load could be estimated from the two sets of moment data. Strain gages were mounted in two positions when using the rigid tube side supports as shown in Figure 9. The outputs of these gages were recorded independently. These data provided an estimate of the longitudinal load through the tube.

TABLE 1.--TRANSDUCERS USED ON TANK CAR HEAD SHIELD CAR-COUPLING IMPACT TESTS

Gage Channel	Type of Transducer	Active Strain Gages per Channel	Location
1 2 3	Strain Gages	Two (wired in bending bridge, active gages on front and back of shield at same location)	Shield (Figure 7)
4	Displacement	N.A.	Shield/Head (Figures 7, 8 and 9)
5 6 7 8	Strain Gages	Two (wired in bending bridges at two locations on each strap support) Two (wired in compression bridges at two locations on each tube support)	Strap Supports, or Tube Supports (Figures 8 and 9)
9 10 11 12	Strain Gages	Two (wired in bending bridge)	Support Angle, Right Side, Between Side Sill and Shield (Figure 10)
13 14 15 16	Strain Gages	Two (wired in bending bridge)	Support Angle, Right Side, between Shield and Stub Sill (Figure 10)
17 18 19 20	Strain Gages	Two (wired in bending bridge)	Support Angle, Left Side, between Side Sill and Shield (Figure 11)
21 22 23 24	Strain Gages	Two (wired in bending bridge)	Support Angle, Left Side, between Shield and Stub Sill (Figure 11)
25	Coupler Force	N.A.	Anvil Car on Hammer Car Test. Hammer Car on Free to Roll and Anvil Car Tests

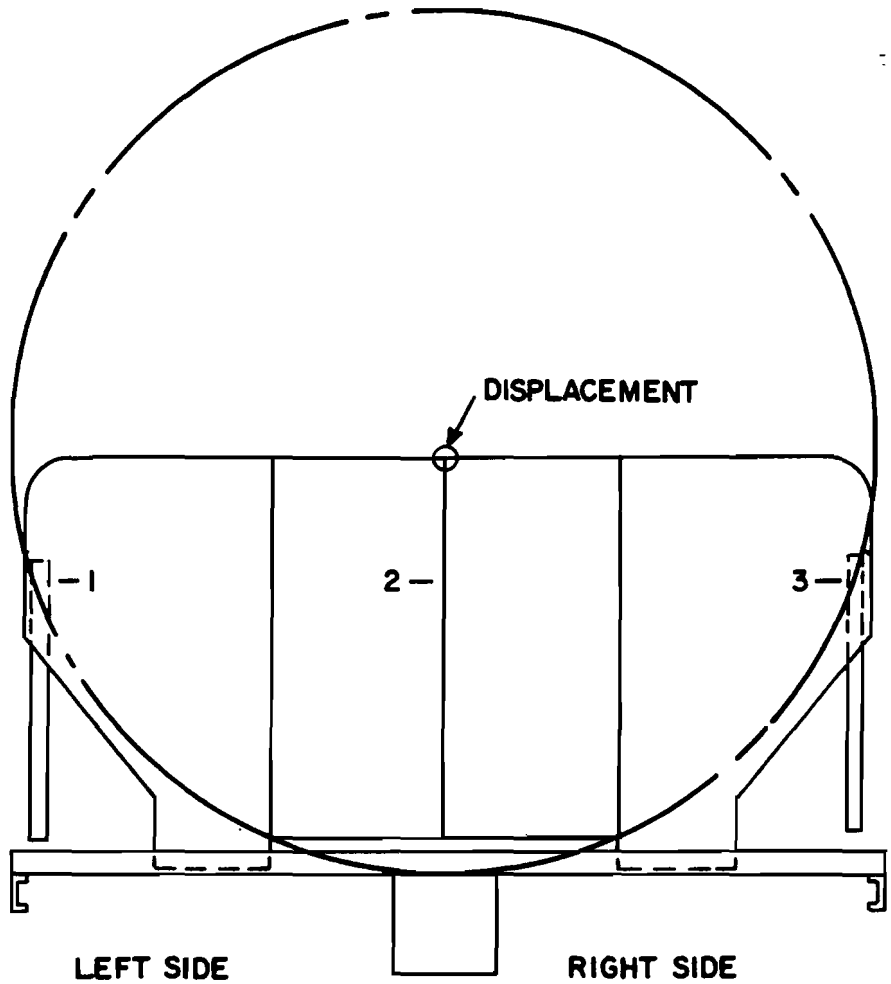

FIGURE 7. GAGE PLACEMENT ON FRONT OF SHIELD. Gages front and back at positions 1, 2, and 3 wired as bending bridges.

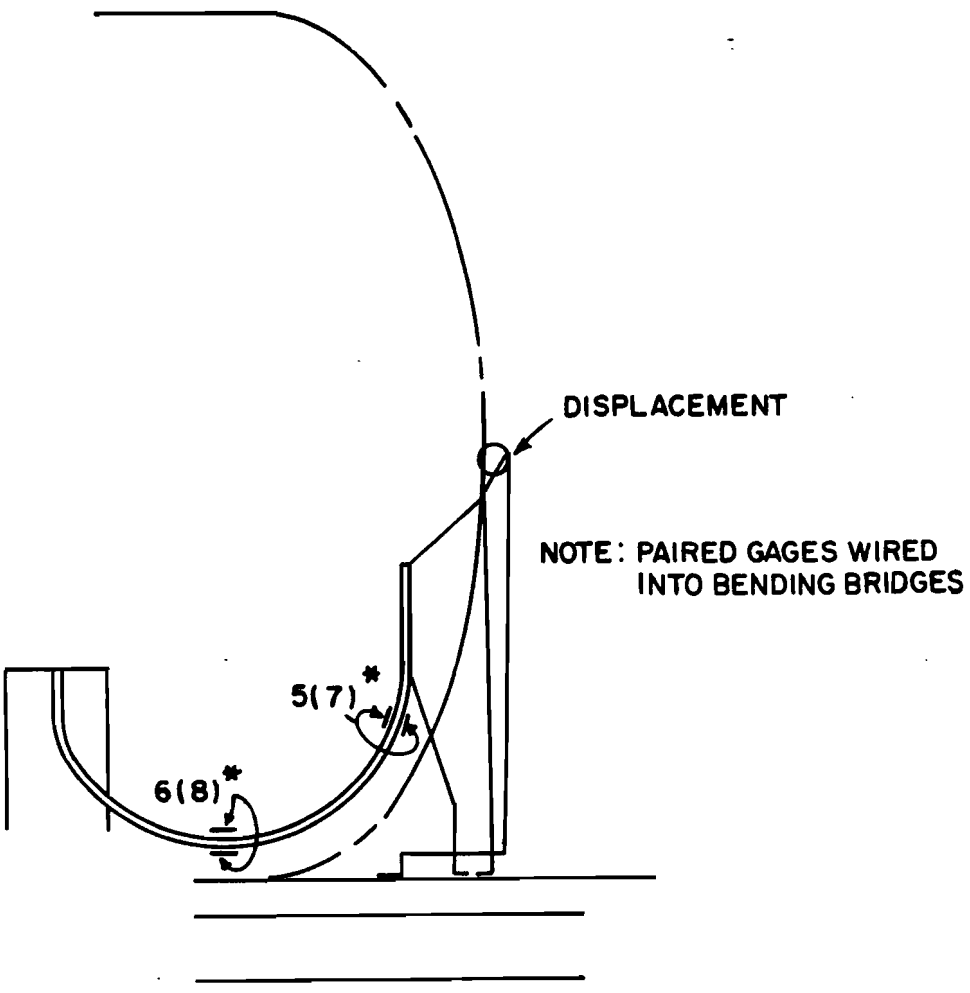

FIGURE 8. GAGE LOCATIONS ON STRAP SUPPORTS.
*View shown is for left side of car, right side gages are Numbers 7 and 8.

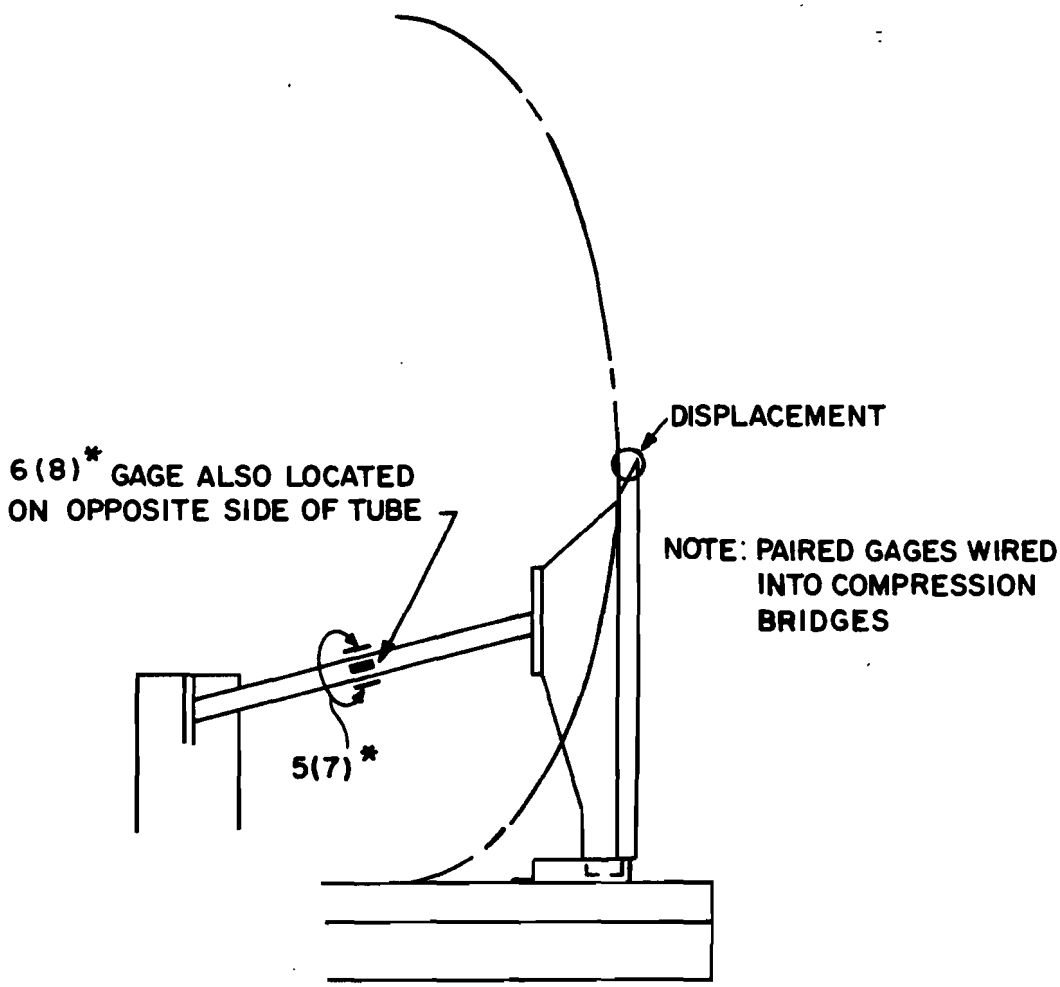

FIGURE 9. GAGE LOCATIONS ON TUBE SUPPORTS.
*View shown is for left side of car, right side gages are Numbers 7 and 8.

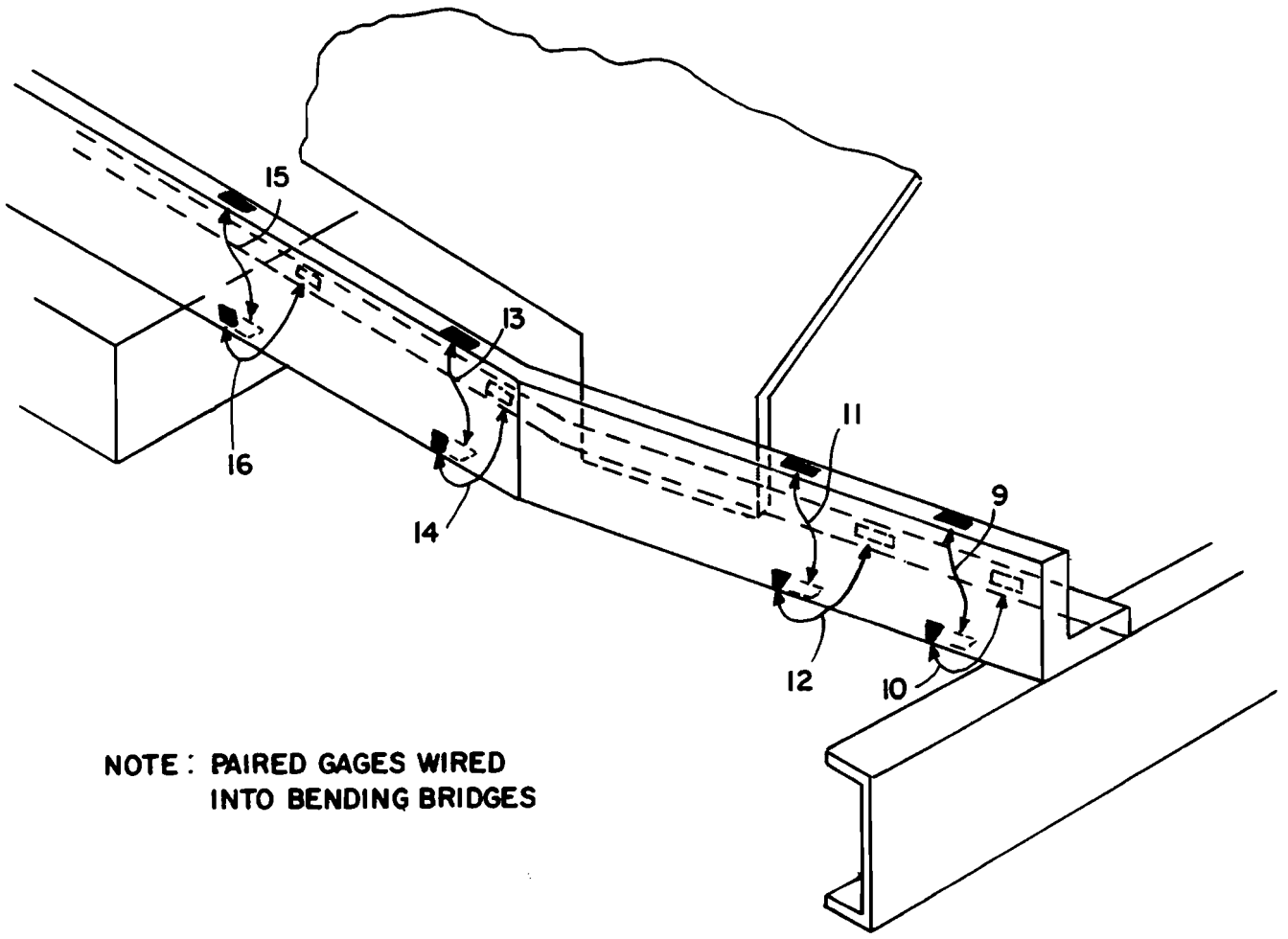

FIGURE 10. GAGE PLACEMENT DETAIL FOR HEAD SHIELD SUPPORT ANGLE ON RIGHT SIDE OF CAR.

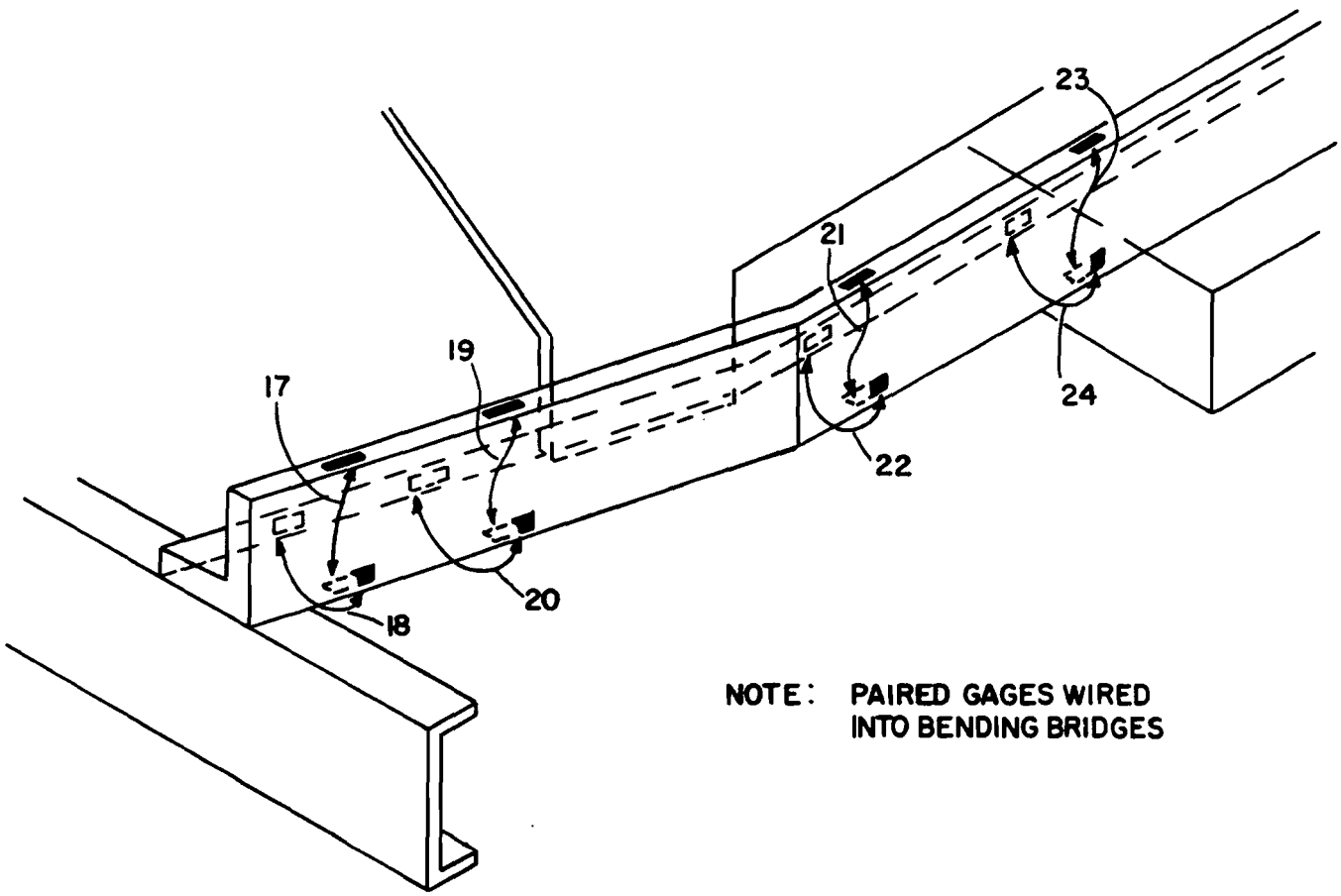

FIGURE 11. GAGE PLACEMENT DETAIL FOR HEAD SHIELD SUPPORT ANGLE ON LEFT SIDE OF CAR.

Strain gages were mounted on the support angle between the stub sill and the shield supports, and the side sill and shield support, on both sides of the car (Figures 10 and 11) to determine the bending moments in the angle in both the horizontal and vertical planes parallel to the member. By knowing the differences in the bending moments between sets of gages it was possible to calculate both the vertical and horizontal shear in the member, and thus define the interfacial loads between the shield and the stub sill and the shield and the side sill.

Movement of the shield with respect to the car was monitored by a displacement gage (Figures 7, 8 and 9) between the top of the shield and the tank head. A dynamometer coupler was used to provide a record of coupler force as a function of time during the impact.

High speed motion pictures were taken with one camera operating at approximately 500 fps, and another operating at 64 fps was positioned to obtain a side-on view of the shield. Two cameras operating at 64 fps were positioned to provide additional views of the shield. An additional camera operating at 18 fps recorded a side-on view of the impact.

The data were recorded on magnetic tape at 7.5 ips. Two recorders used for this purpose were located within the Miner Enterprises Inc., instrumentation facility adjacent to the test track. These recorders were connected to the transducers on the tank car through a 1500 ft long hard-wire system. The cables are hung from trolleys adjacent to the test track so that they can follow the movement of the car.

2.3 Test Operations

Six series of impact tests were performed: one with strap (flexible) side supports; one with the tube (rigid) side supports utilizing the anvil car test procedure; one with the tube support system utilizing the free-to-roll test procedure; and one series each with the tube, strap, and strap with shock absorber support systems utilizing the hammer car test procedure.

The first test series was performed July 28, 1975 using the anvil car test procedure and the strap side supports. The impact speeds and associated maximum coupler forces are:

Impact Velocity (mph)	Maximum Coupler Force (1000 lb)
3.28	201
4.03	294
4.90	332
5.90	719
7.06	1065

The second test series was performed July 29-30, 1975 utilizing the anvil car test procedure and the tube side supports. The impact speeds and associated maximum coupler forces are:

Impact Velocity (mph)	Maximum Coupler Forces (1000 lb)
3.06	205
3.13	213
4.03	230
4.97	346
6.00	801
7.09	1152
7.79	1286

The third impact series was performed July 31, 1975 utilizing the free-to-roll test procedure and the tube side supports. The impact speeds and associated maximum coupler forces are:

Impact Velocity (mph)	Maximum Coupler Force (1000 lb)
3.08	195
3.98	261
3.11	205
4.90	298
5.96	595
7.07	977
7.73	1155

The fourth impact series was performed August 4, 1975 utilizing the hammer car test procedure and the tube side supports. The impact speeds and associated maximum coupler forces are:

Impact Velocity (mph)	Maximum Coupler Force (1000 lb)
3.34	208
4.21	221
4.17	247
4.18	312
4.20	290
5.10	304
5.13	283
6.08	421
7.00	946
7.60	1099

The fifth impact series was also performed August 4, 1975 utilizing the hammer car test procedure and the strap side supports. The impact speeds and associated maximum coupler forces are:

Impact Velocity (mph)	Maximum Coupler Force (1000 lb)
3.26	217
4.24	302
5.13	351
6.05	449
7.08	975
7.63	1108

The sixth impact series was performed August 5, 1975 utilizing the hammer car test procedure and the strap with shock absorber side supports. The impact speeds and associated maximum coupler forces are:

Impact Velocity (mph)	Maximum Coupler Force (1000 lb)
3.27	213
4.19	306
5.07	384
6.02	470
6.94	994
7.60	1105

3. TEST RESULTS - CAR COUPLING IMPACTS

3.1 Dynamic Response Phenomena

The results from the car-coupling impact tests showed that the stresses within the shield itself and the loads within the side supports were well below levels where fatigue damage would be expected, but that the angle which supported the weight of the shield was highly stressed. The high stresses in the angle were due to the excitation of vertical vibratory motions. As expected, the transient displacement of the shield with the strap supports was greater than the shield with the tube supports.

The anvil car tests showed high loads in the supporting structure of the shield which were due in part to the dynamic response sensitivity of the shield to the displacement of the tank car as it is struck by the impacting car. Initially it was believed that the anvil car test would be less severe than the hammer car test. The tests revealed, however, that the maximum loads recorded at comparable impact speeds were higher on the anvil car tests than on the hammer car tests. On the hammer car tests the maximum response phenomena (displacement, strain, load, etc.) almost always occurred during the first period of vibration of the fundamental mode. Each succeeding peak showed a decay in the signal level from the preceeding peak. Data from the anvil car tests showed that the peak values of the response parameters increased in intensity from one to three periods of vibration of the fundamental mode. This was followed by a decay in peak values. The data from these channels were subsequently recorded as the local peak value of the first three or four maxima coinciding with the fundamental frequency of shield response.

The large displacements and strains measured on the anvil car tests were somewhat surprising in view of the fact that the shield equipped car is initially at rest and that it is displaced a relatively short distance, on the order of 6 to 30 inches, from the effects of the impact by the hammer car. A detailed study of

the motions of the struck car suggests that the start-stop motion, which is imparted to the car by the impact, is in phase with the fundamental mode of longitudinal oscillation of the shield and that this tends to amplify the shield displacement.

3.2 Data Presentation

3.2.1 Shield Displacement—Figures 12 and 13 compare the maximum longitudinal displacement of the top of the shield as a function of impact velocity for both strap and tube side supports. As expected, the strap support allows approximately twice the deflection of the shield as the tube support. The frequencies for the fundamental longitudinal mode of vibration were 5.8 Hz when the strap supports were used, and 10.8 Hz when the tube supports were used. Note that the use of the shock absorbers with the strap side supports reduced the maximum displacement somewhat.

3.2.2 Shield Plate Strains—The greater flexibility provided by the strap support results in lower strains in the shield itself. This is shown by the data presented in Figures 14 and 15. Figure 14 compares maximum horizontal strains measured at the center of the shield for both strap and tube side support systems as a function of impact velocity. Note that all strains are well below the elastic limit of the material (approximately 1,300μ inch/inch and that the strains with the strap support are approximately one-half of those with the tube support.

Figure 15 also includes a comparison of the effect of using shock absorbers with the strap supports. This device increases the strains associated with the first peak (when compared to the straps alone) and results in a more rapid decay on succeeding peaks as shown by the second peak comparison.

3.2.3 Forces Transmitted Through Side Supports—The magnitude and character of the forces transmitted from the shield to the car structure are of particular interest for the evaluation of the shield structural system. There are two paths for these loads: through the side supports and through the horizontal support angle.

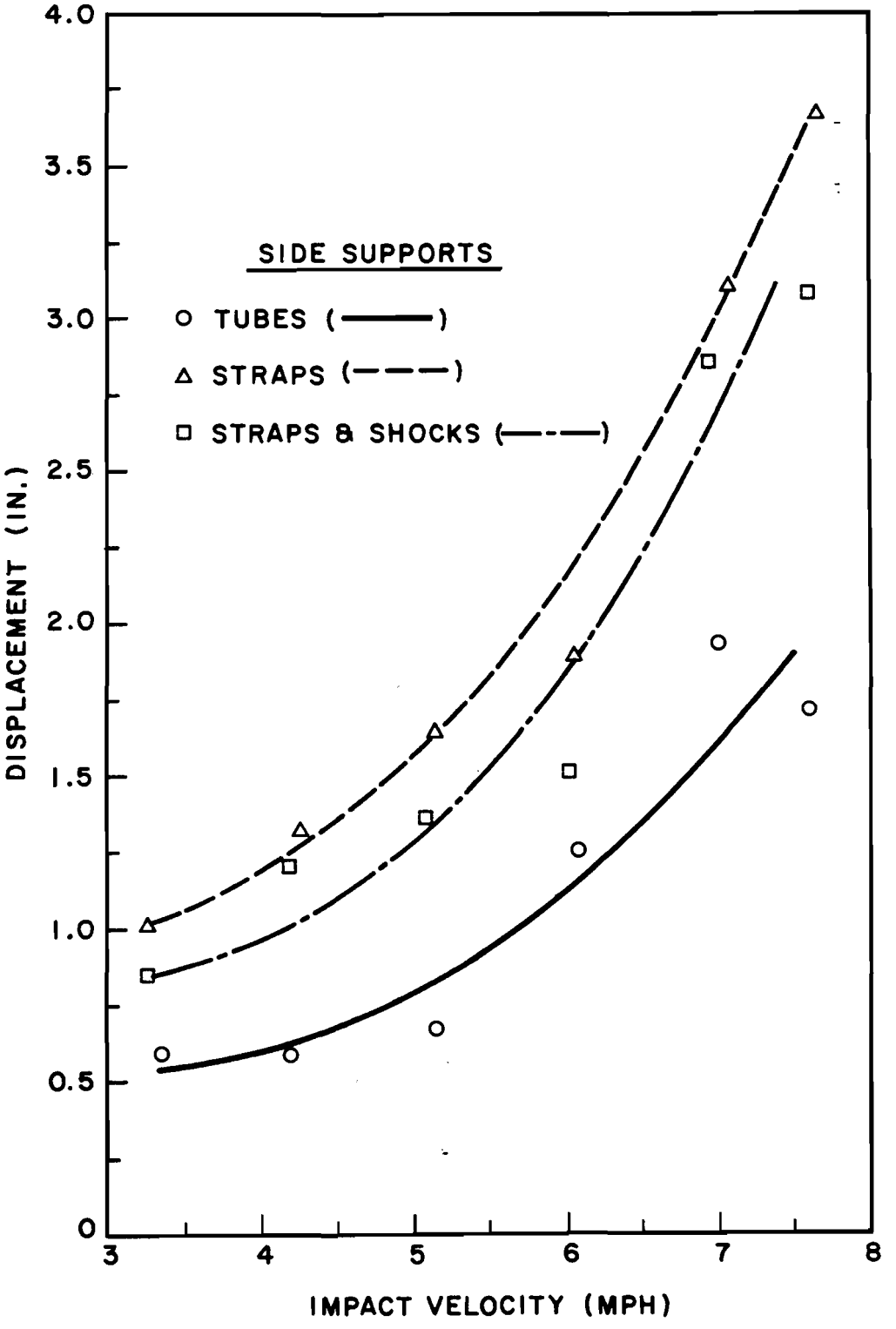

FIGURE 12. MAXIMUM DISPLACEMENT OF CENTER OF SHIELD, HAMMER CAR TESTS.

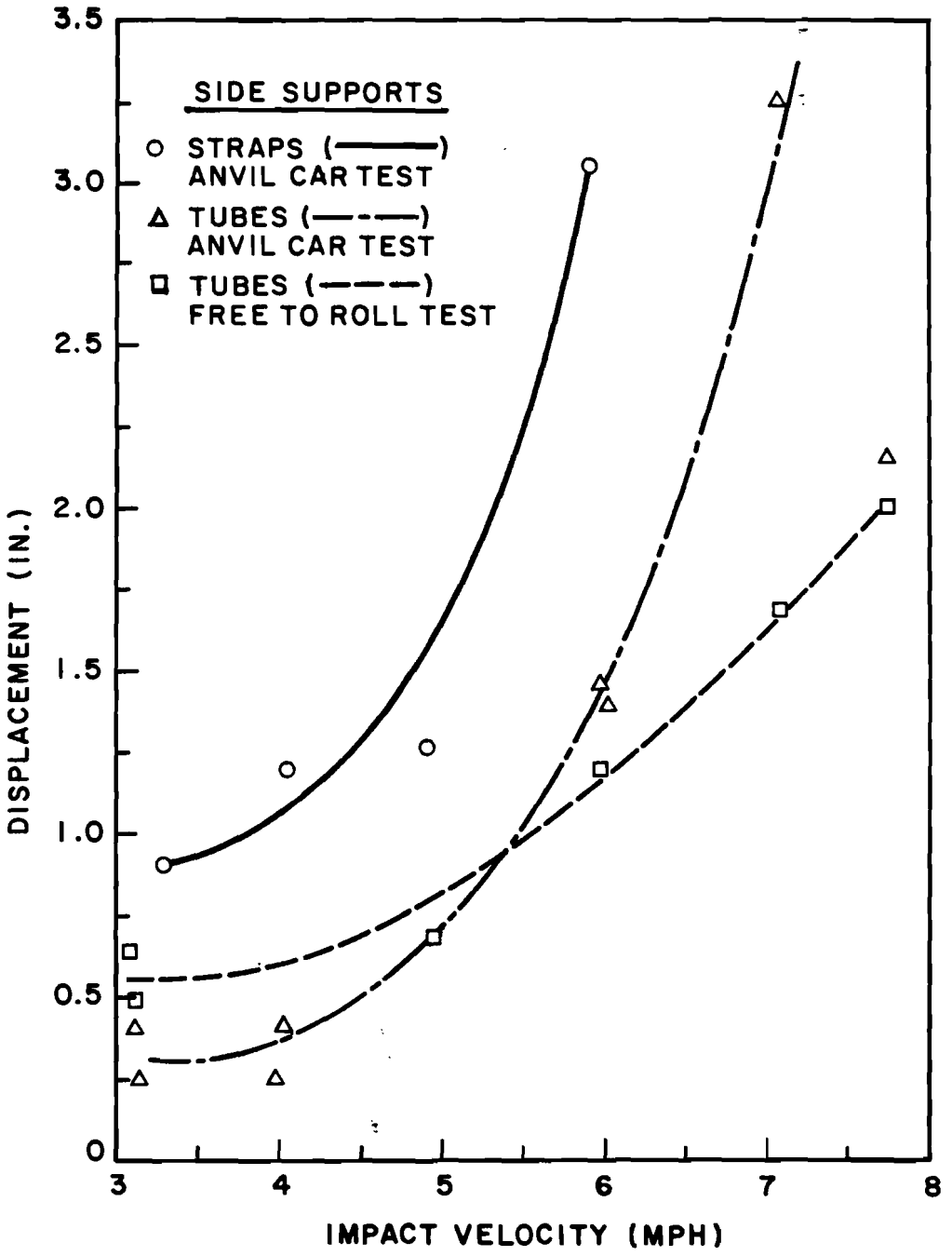

FIGURE 13. MAXIMUM DISPLACEMENT OF CENTER OF SHIELD, ANVIL CAR TESTS.

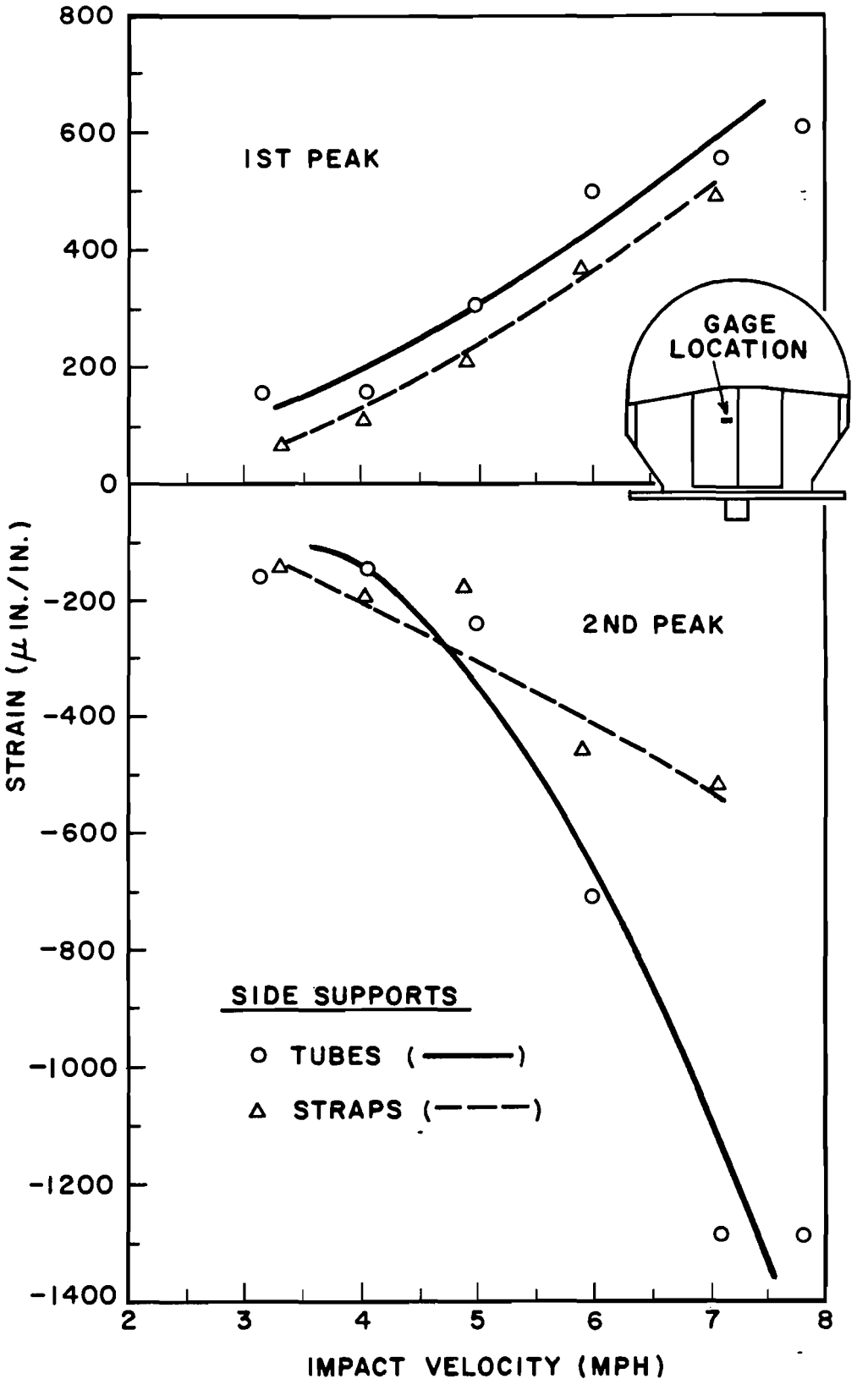

FIGURE 14. MAXIMUM HORIZONTAL STRAINS MEASURED ON GAGES AT CENTER OF SHIELD, ANVIL CAR TEST.

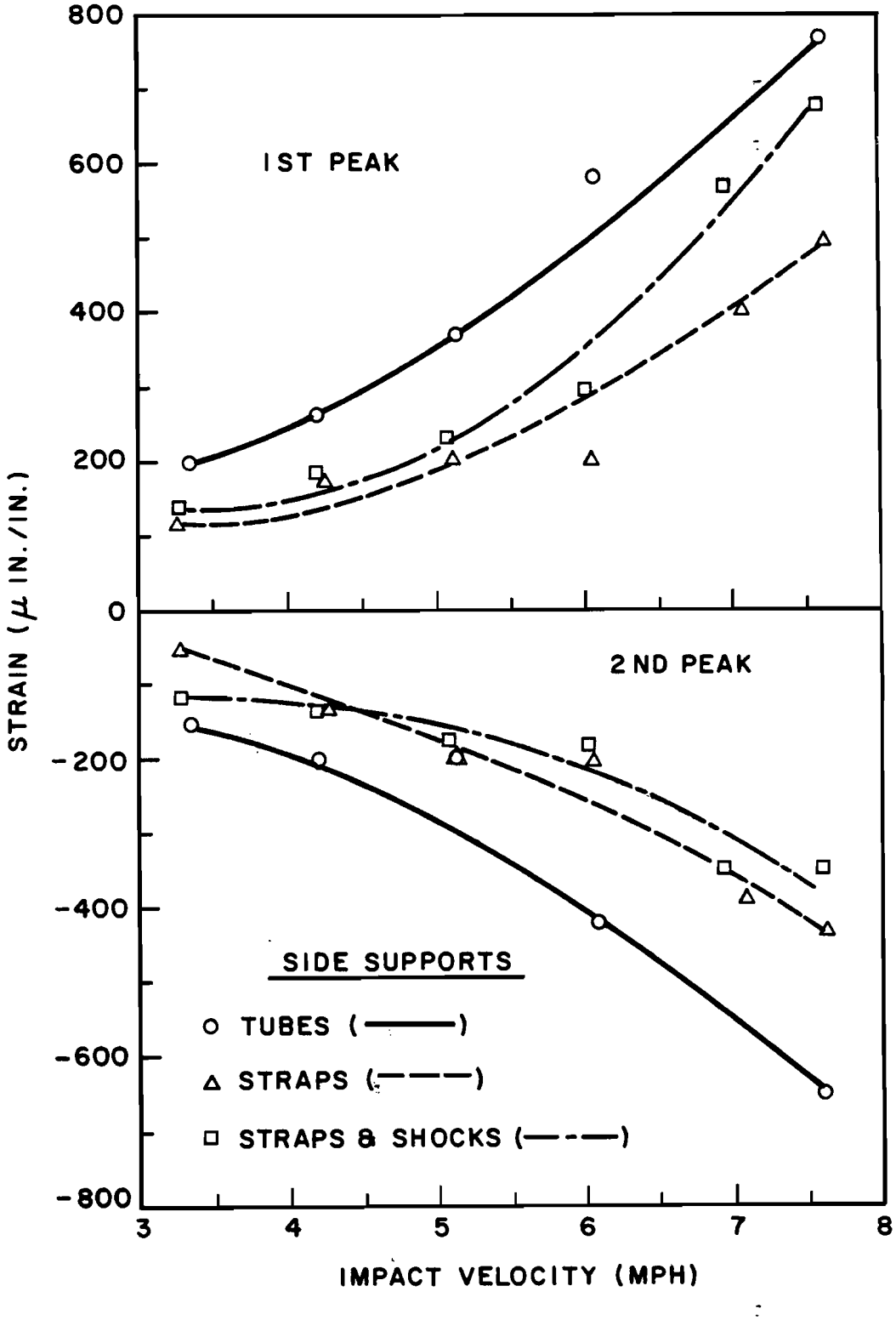

FIGURE 15. MAXIMUM HORIZONTAL STRAINS MEASURED ON GAGES AT CENTER OF SHIELD, HAMMER CAR TESTS.

The data presented in Figures 16 through 19 show the magnitude of the maximum transient loads exerted on the tank car bolster through both the strap and tube side support systems. Figures 16 and 17 show the maximum longitudinal load acting through the strap supports as a function of impact velocity. The forces are larger on the left side of the shield (Figure 17) where the hand brake is located. The elevation of the line-of-action of the longitudinal load was calculated and found to be relatively constant over the range of impact velocities. The distance of the line of action of the longitudinal load above the base of the shield averaged approximately 38 inches on the left side and 52 inches on the right side of the shield.

Figures 18 and 19 show the maximum longitudinal loads acting through the tube supports as a function of impact velocity. Note that the loads are from two to six times higher than corresponding loads transmitted through the strap supports. First and second peak data are plotted to show the tendency for the second peak loads to exceed initial peaks on the anvil car tests.

The capacity of the tank car bolster to withstand the longitudinal loads from the shield side supports has been calculated to be in excess of 10,000 lb so that the maximum forces from either the tube or strap side supports are within acceptable limits.

3.2.4 Forces Transmitted Through Support Angle—The second path of load transfer between the shield and car is through the horizontal angle which supports the weight of the shield. This angle is welded to the side sills and the stub sill so that the loads are transferred into the structure of the car at these points.

Load transfer through this member under car impact conditions involves complex response phenomena. The primary load is a longitudinal inertial load, which is reacted both by axial tensile and shear forces in the angle. The axial tensile forces are due to the bend in the outer portions of the angle with respect to a transverse reference line. The shear forces are due

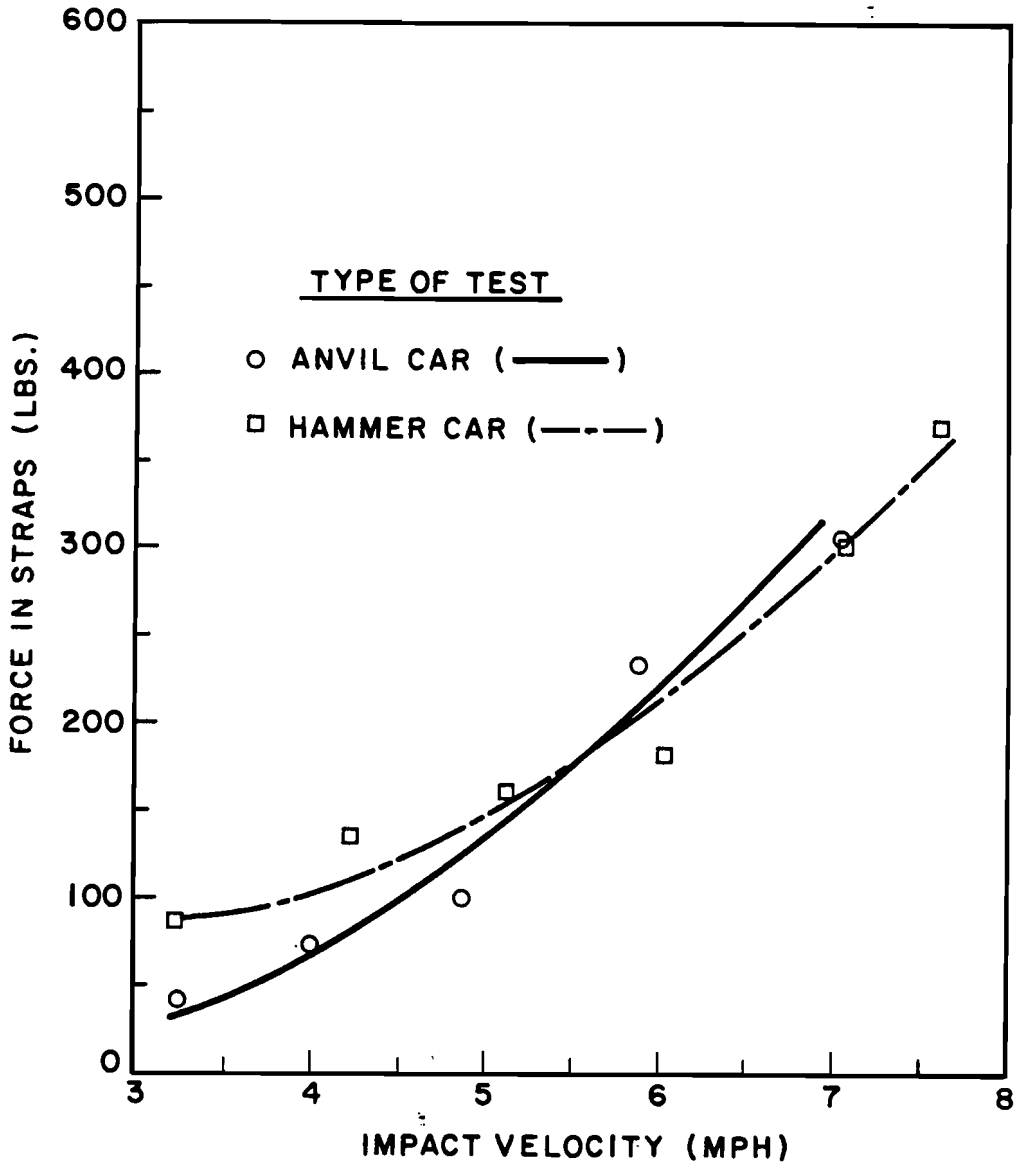

FIGURE 16. MAXIMUM LONGITUDINAL FORCE THROUGH RIGHT STRAP SIDE SUPPORT.

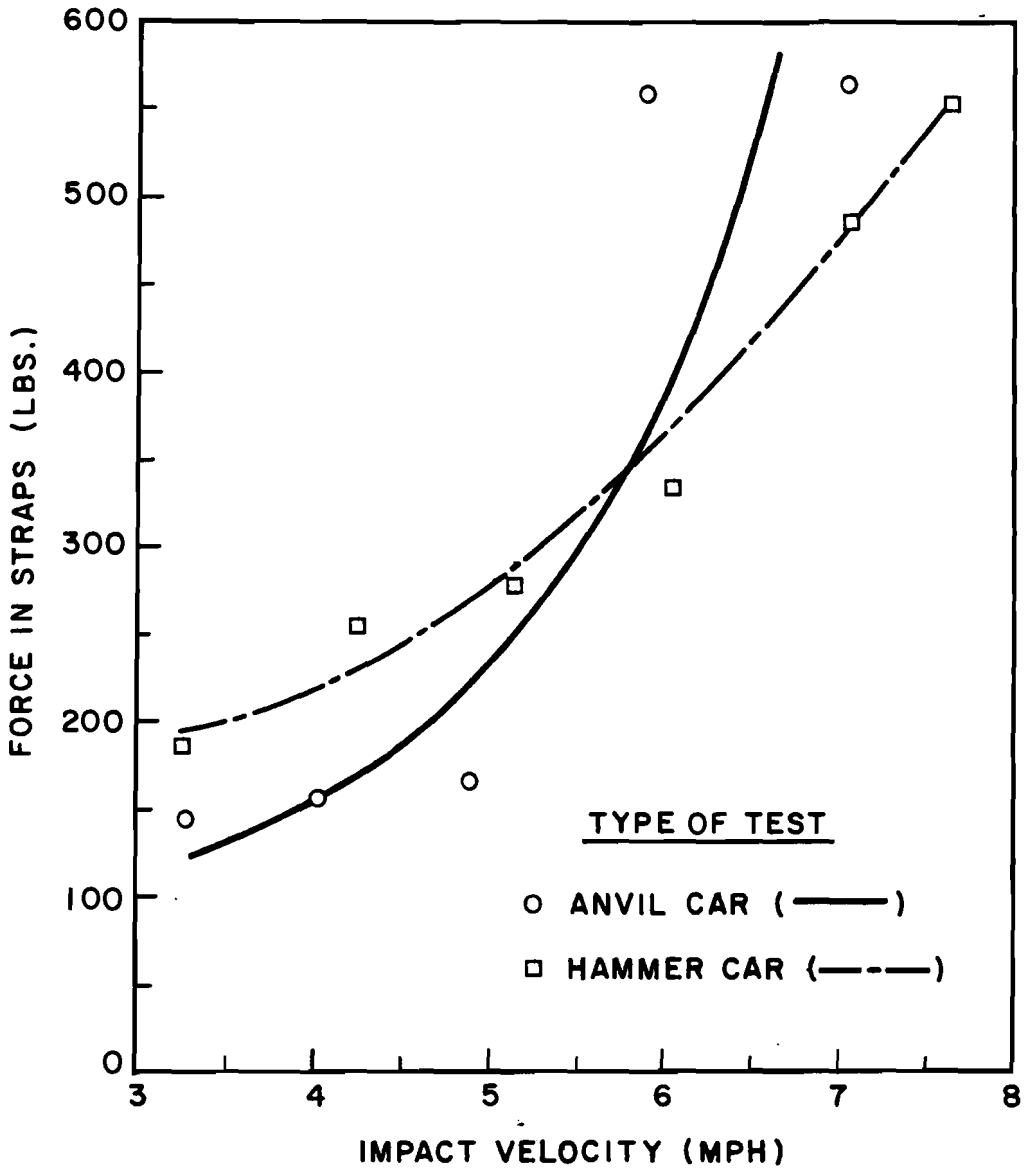

FIGURE 17. MAXIMUM LONGITUDINAL FORCE THROUGH LEFT STRAP SIDE SUPPORT.

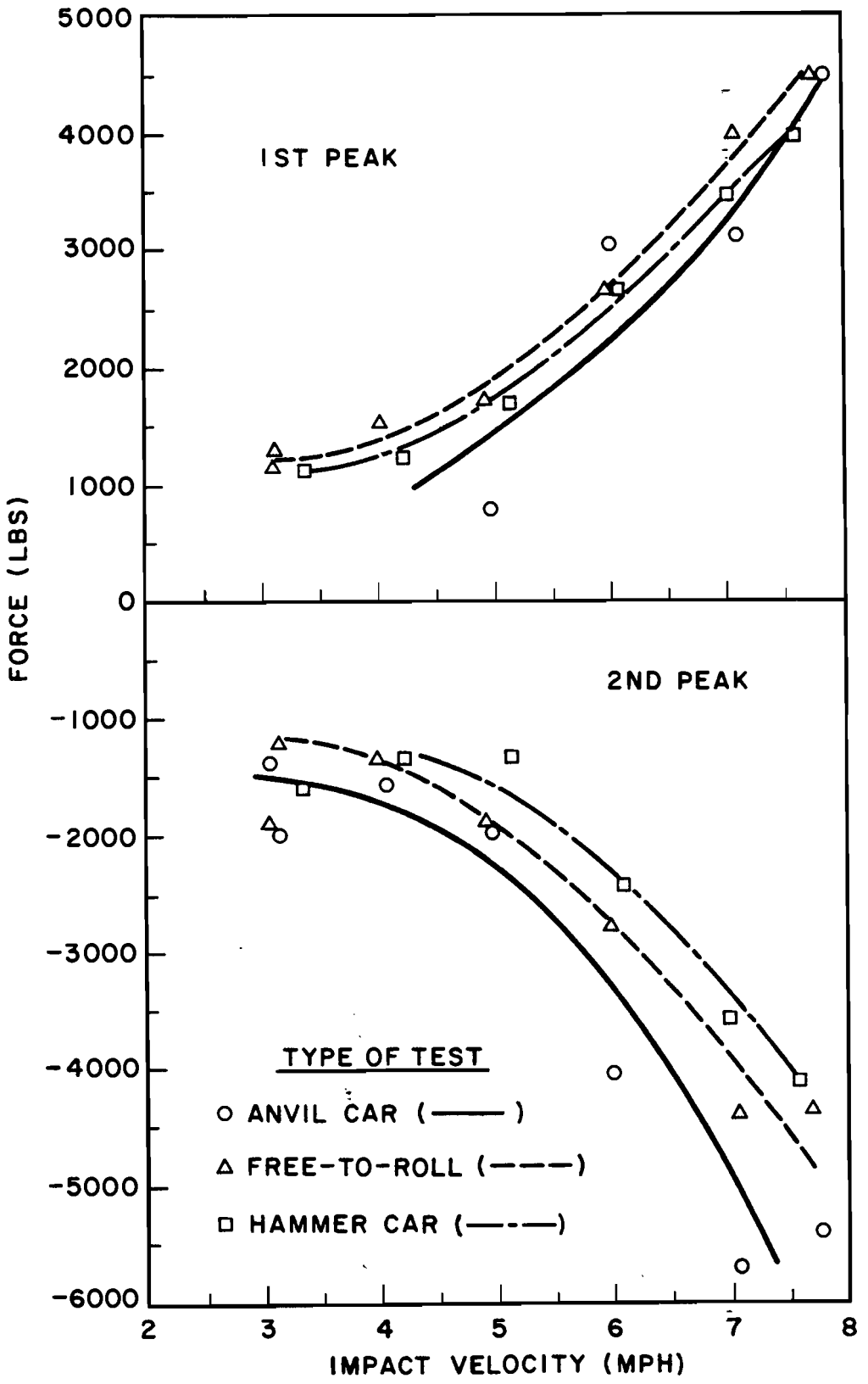

FIGURE 18. MAXIMUM LONGITUDINAL FORCE IN LEFT TUBE SUPPORT.

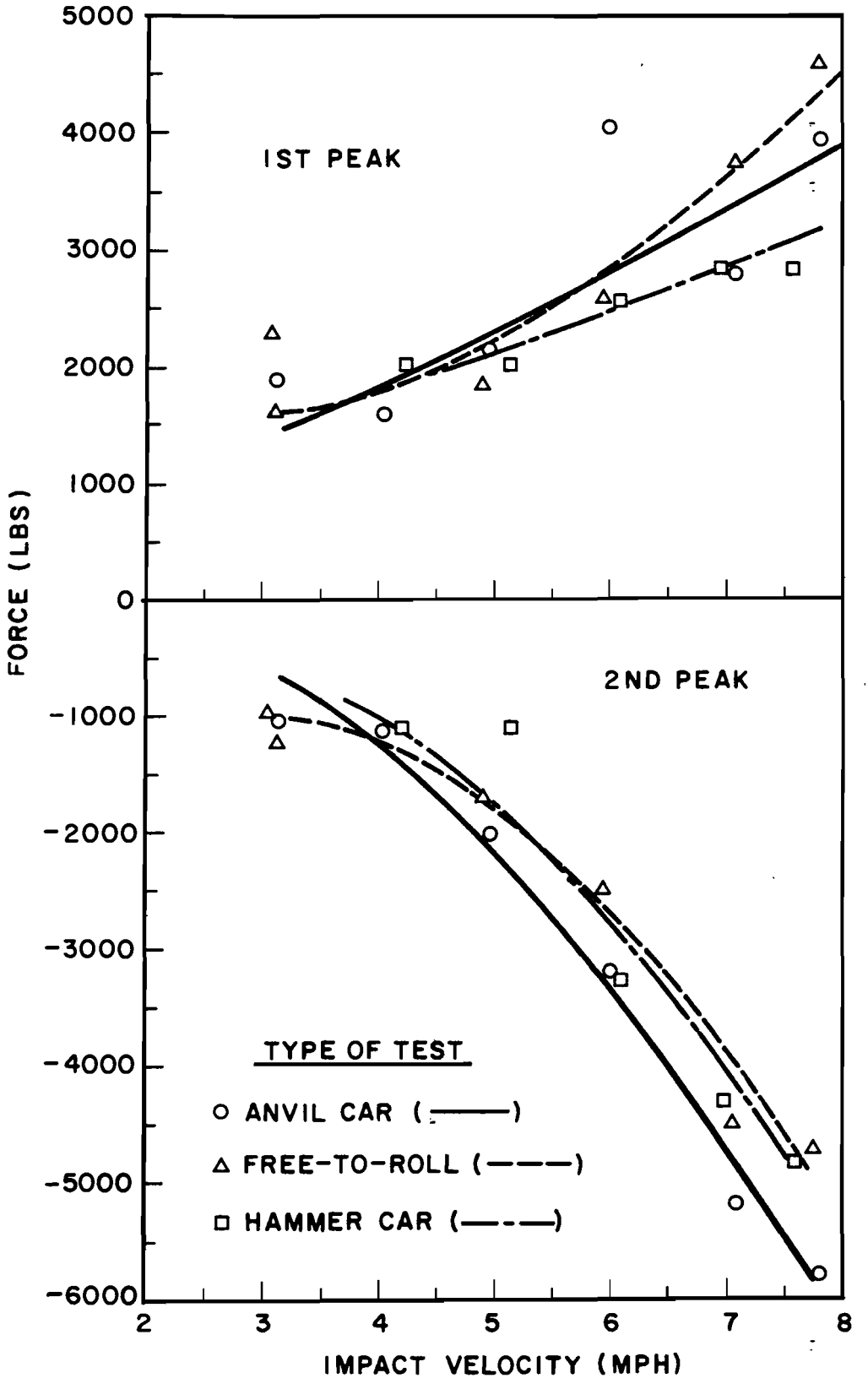

FIGURE 19. MAXIMUM LONGITUDINAL FORCE IN RIGHT TUBE SUPPORT.

to the rigid connections at the side sill and stub sill interfaces and would result from bending of the angle.

Load transfer to the stub sill and side sills through shear in the angle was measured by installing four sets of bending bridges between the shield attachment and the side sills, and four sets of bending bridges between the shield attachment and the stub sill (Figures 10 and 11). These gages permitted the determination of bending moments on the principal axes of the angle at eight locations, which allowed for the calculation of shear forces between adjacent sets of gages. These shear forces were resolved into longitudinal and vertical components.

Under car impact it was observed that the longitudinal displacement of the shield was coupled into a vertical motion which displaces the support angle in a vertical direction. This motion was most pronounced with the strap side supports. The shear forces in the angle associated with this phenomenon were calculated by processing the analog data from the sets of strain gages on the support angle on a Nova 1220 minicomputer. The procedure included digitizing the signal from each bending bridge, performing transformations to determine the moments about the principal axes, computing the shear loads with respect to the principal axes, and combining the longitudinal and vertical components of the shear loads.

Figures 20 and 21 show results from these calculations. Maximum shear force data in the angle are plotted as a function of impact velocity. Note that the load transfer to the stub sill, Figure 21, is larger in all cases than load transfer to the side sill, Figure 20. This is as expected because the stub sill is a more rigid member of the tank car structure than the side sill. Also notice that in almost every case the maximum vertical shear force is at least twice the maximum horizontal shear force. This shows the pecularities of the dynamic response of the shield support system whereby the primary horizontal inertial loads are coupled into strong vertical motions with accompanying high vertical loads on the support angle. The figures also show that the loads

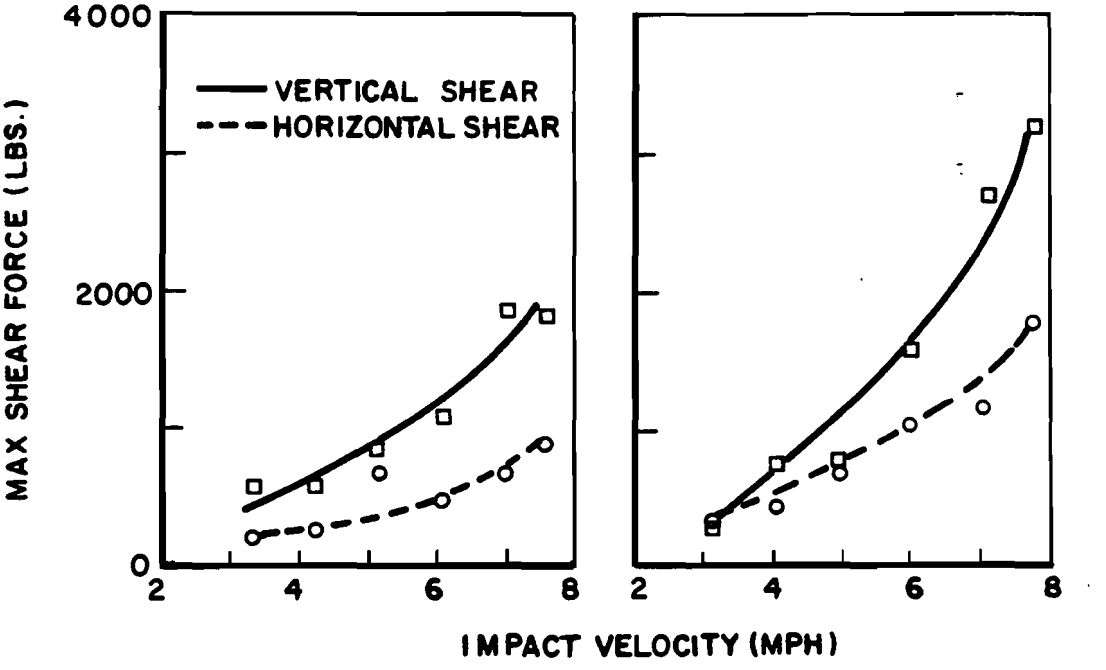

(a) HAMMER CAR TEST (TUBES) (b) ANVIL CAR TEST (TUBES)

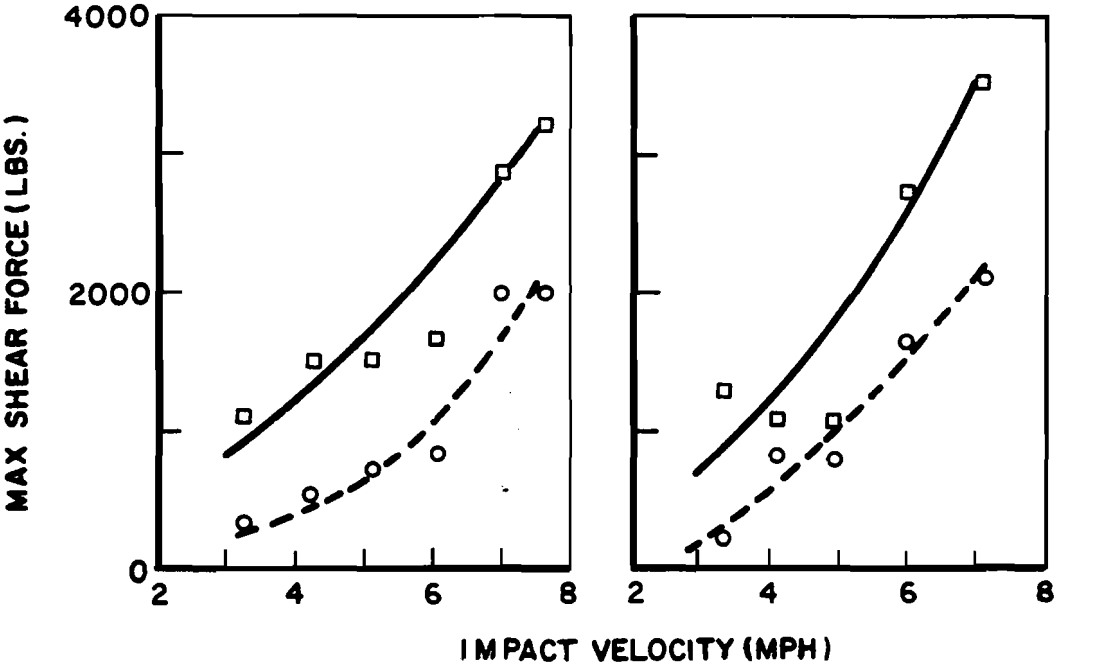

(c) HAMMER CAR TEST (STRAPS) (d) ANVIL CAR TEST (STRAPS)

FIGURE 20. MAXIMUM SHEAR FORCE TRANSFER THROUGH SUPPORT ANGLE TO SIDE SILL.

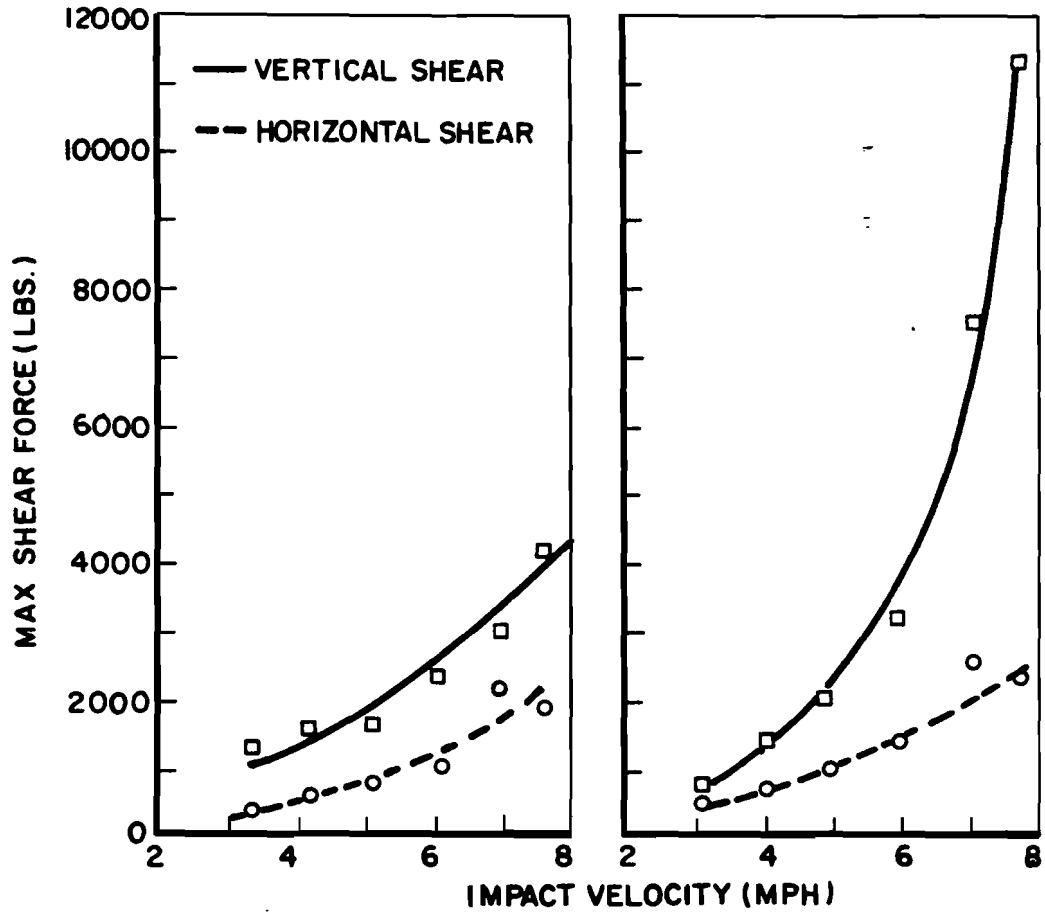

(a) HAMMER CAR TEST (TUBES) (b) ANVIL CAR TEST (TUBES)

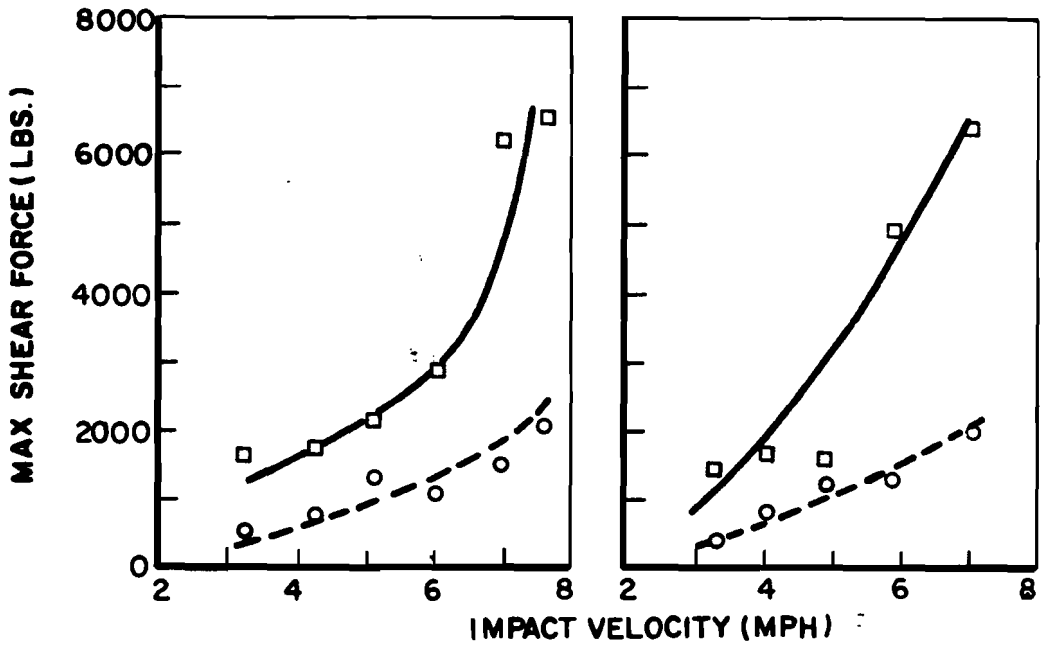

(c) HAMMER CAR TEST (STRAPS) (d) ANVIL CAR TEST (STRAPS)

FIGURE 21. MAXIMUM SHEAR FORCE TRANSFER THROUGH SUPPORT ANGLE TO STUB SILL.

associated with the tube side supports are generally below comparable loads associated with the strap side supports except in the case of the highest force measured on any of the tests, namely the case shown in Figure 21b where the data from the anvil car tests are plotted. In most cases the difference in shear force is small. The data plotted in the figures also show that the hammer car test generally results in smaller loads than comparable anvil car tests.

3.3 Fatigue Analysis

Results from the analysis of shear transmission through the support angle showed that the highest forces were transferred between its connections to the shield and the stub sill. The maximum strains associated with this load-transfer occurred at the top of the vertical leg of the angle adjacent to the stub sill. Having identified these positions (gage channels 15 and 23) as the most critical positions from the standpoint of possible fatigue damage, the rate of accumulation of fatigue damage at this location during car coupling impacts was determined.

This information was related to the anticipated life of the car through statistics (Ref. 3), stating the average number of car coupling impacts per year for this class of equipment, and the distribution of velocities over which these impacts occur. These data are summarized in Table 2. An average of 62.5 car coupling impacts per year is predicted. The events listed in this table refer to switching movements. Normally there would be two primary coupling impacts associated with each event. For example, when a car is humped in a classification yard it will strike into standing cars and in addition, the next car humped will strike it leading to a second coupling impact.

Data from one of the anvil car tests, Test Series 2, and one of the hammer car tests, Test Series 4, were utilized to determine the number and magnitude of strain cycles associated with various car-coupling impact velocities. The oscillographic traces of the strains occurring at the critical location were analyzed for each

impact. The strain cycles were counted according to the rainflow format, which identifies full cycles by their maximum and minimum values. Strain cycles were counted until the strain peaks decayed to a value below the estimated fatigue limit. The data from this analysis are summarized in Tables 3 and 4 where the number of strain cycles within different strain ranges are shown for various impact velocities. These data were used in conjunction with the velocity distribution data, Table 2, to calculate the number of anticipated strain cycles per year as a function of strain amplitude.

TABLE 2.—AVERAGE NUMBER OF YARD COUPLING IMPACTS PER YEAR (REF. 3)

Speed Range (mph)	Average Number of Coupling Impacts per Year
0 to 2	1
2 to 3	3
3 to 4	9
4 to 5	13
5 to 6	15
6 to 7	10
7 to 8	6
8 to 9	3
9 to 10	1.5
10 to 11	1
	62.5

An estimate of the fatigue curve for SAE 1028 steel, which is representative of the structural steel which would be used in the head shield support construction, was developed from the Manson-Coffin and Basquin laws (Ref. 4).

$$\Delta\varepsilon = 3.5 \frac{\sigma_u}{E} (N_f)^{-.12} + (D)^{.6} N_f^{-.6}$$

where $D = \ln \frac{1}{1-RA}$

RA is reduction in area

σ_u is the ultimate strength

E is the modulus of elasticity

N_f is the cyclic fatigue life

$\Delta\varepsilon$ is the total (plastic and elastic) strain range

The fatigue life curve developed from this expression is shown in Figure 22.

TABLE 3.—SUPPORT ANGLE STRAIN CYCLES ASSOCIATED WITH ANVIL CAR TESTS

Impact Speed (mph)	Strain Range (min/max; μ in./in.	Cycles per Impact
7.8	-3375/4140	1
	-2835/4140	1
	-2295/2565	1
	-1755/135	1
	-1215/1485	1
	- 945/3105	1
	- 675/945	1
	- 675/675	2
	- 675/405	2
	- 405/405	1
7.1	-2835/2835	1
	-2295/2835	1
	-1215/1215	2
	- 945/945	1
	- 675/945	2
	- 405/1485	1
	- 405/405	2
6.0	-1755/1755	1
	-1215/1215	1
	-1215/945	1
	- 675/675	2
	- 675/405	1
	- 405/675	1
	- 675/135	1
	- 405/405	2
5.0	- 405/945	1
	- 405/405	2
	- 135/675	2
4.0	- 425/425	3

TABLE 4.–SUPPORT ANGLE STRAIN CYCLES ASSOCIATED WITH HAMMER CAR TESTS

Impact Speed (mph)	Strain Range (min/max; μ in./in.)	Cycles per Impact
7.6	-2015/2295	1
	- 945/1215	1
	- 675/945	2
	- 675/675	1
	- 135/675	1
7.0	-2015/1755	1
	- 675/675	1
	- 405/675	1
	- 405/405	1
	- 135/675	1
6.1	- 405/945	1
	- 135/675	1

The percentage of useful fatigue life which is expended per year as a result of the car coupling impacts was then calculated utilizing the linear damage law. For this calculation it was assumed that each coupling impact event involves two sets of strain cycles. One like those measured on the hammer car tests (Table 3) and one like those measured on the anvil car tests (Table 4). Results from the calculation indicate a yearly expected fatigue damage at this point in the support angle of 0.0028. This implies an anticipated service life of 360 years.

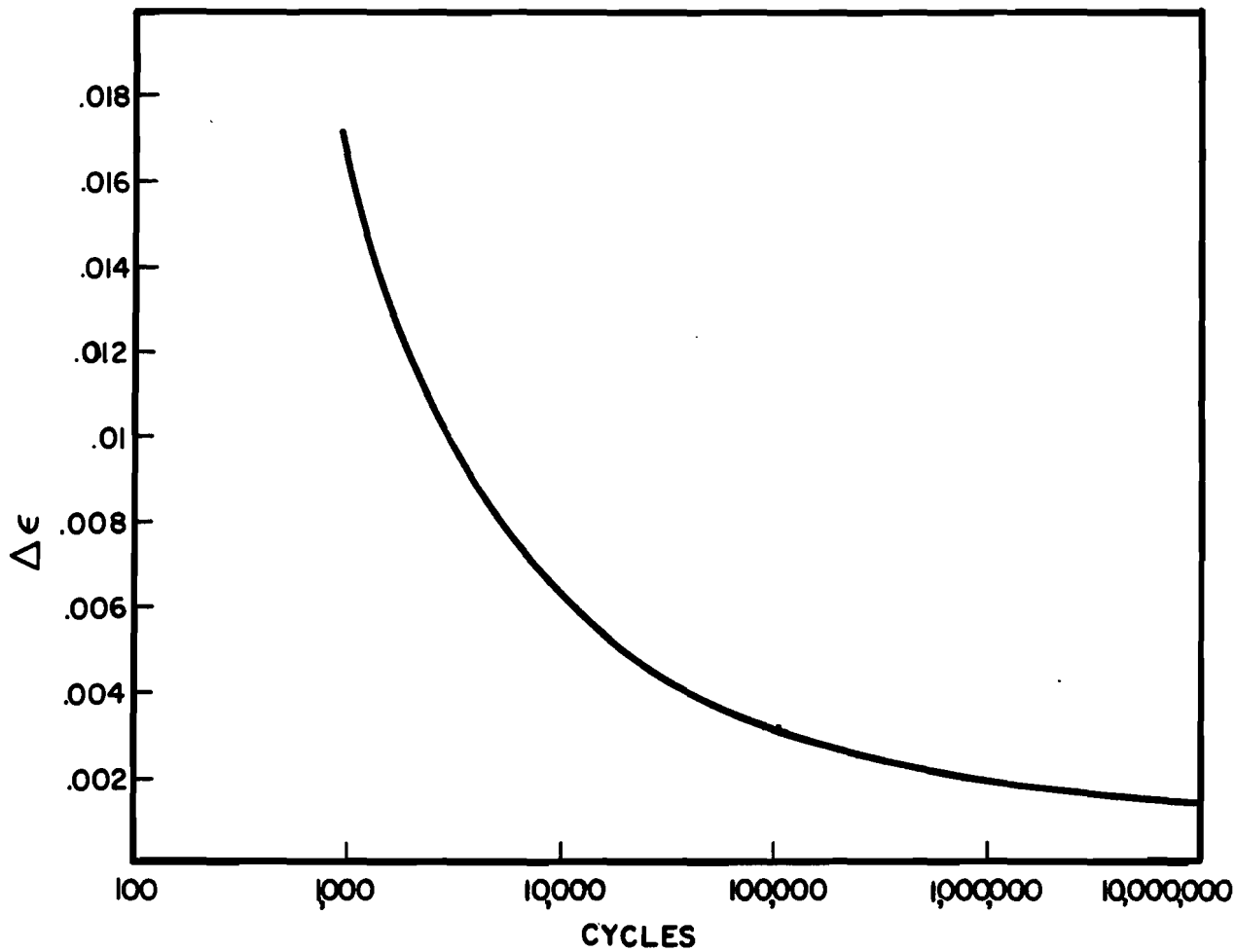

FIGURE 22. ESTIMATED FATIGUE CURVE FOR SAE 1028 STEEL.

4. TEST PLAN - OVER-THE-ROAD

4.1 Objective

The objectives of the over-the-road tests were to determine the loads acting on the prototype tank car head shield when the car is subjected to typical over-the-road conditions, and determine if these loads will cause fatigue damage to the head shield and the points of its attachment to the car over the anticipated service life of the car.

4.2 Test Procedures

The prototype head shield with the tube side supports was installed on tank car RAX 203. The car and shield were instrumented with transducers to monitor strains on the support angle, side supports and shield, displacement of shield, side frame and side bearing forces, and car acceleration. Data from the transducers were recorded continuously during the over-the-road movement. Recording equipment, signal conditioning equipment and test personnel were housed in a caboose coupled to the end of the tank car on which the shield was installed.

The test consist was positioned at the ends of trains which normally attained speeds over 50 mph. This allowed excitation of the vibrational frequencies associated with various speed ranges. Two round trip runs were made between Homewood and Champaign, Illinois on the main line of the Illinois Central Gulf Railroad. The first run was made with the car empty and the second was made with the car loaded with water to a total rail load of 263,000 lb, which is the maximum rail load allowed for the car.

Instrumentation was applied at the Research and Development Division of Miner Enterprises Inc. Miner personnel installed the gages and provided miscellaneous services to assist IITRI engineers in the preparation of the car for the over-the-road tests.

4.3 Instrumentation

Many of the transducer locations used on the car-coupling impact tests were also used for the over-the-road tests. Table 5 is a list of these transducers. Their locations are shown in Figures 23 to 26. Gage Channels 2, 4, 5, 7, and 13 to 24, are the same as used on the car-coupling impact tests.

In addition to the instrumentation installed on the head shield, the truck at the shield end of the car was equipped with instrumented side frames for the measurement of vertical truck forces (Gage Channels 27 and 28; Figure 25). The truck was also equipped with instrumented side bearings for the measurement of vertical side bearing loads (Gage Channels 29 and 30; Figure 26).

A wheel revolution counter was used to monitor car velocity so that vibrational frequencies, loads, etc., could be correlated with speed (Gage Channel 31). A time code generator was used to establish a time base reference (Gage Channel 32) and a voice channel was used to provide a verbal record of significant events. An accelerometer, sensitive to vertical motions, was mounted vertically on the stub sill to measure rigid body motions of the car (Gage Channel 26; see Figures 23 and 24).

All data were recorded on magnetic tape in analog form at 1.875 ips. Two recorders were used for this purpose. The assignment of data channels to these recorders is given in Table 6. During the tests up to six channels of data could be displayed on an oscillographic record. This permitted the quality of the data signal to be reviewed and also made it possible to identify regions where detailed analysis of the data was warranted.

TABLE 5.—TRANSDUCERS USED ON OVER-THE-ROAD TANK CAR HEAD SHIELD TESTS

Gage Channel	Type of Transducer	Active Strain Gages per Channel	Location
2	Strain Gages	Two (wired in bending bridge, active gages on front and back of shield at same location)	Shield (Figure 23)
4	Displacement	N.A.	Shield/Head (Figures 23,24)
5 7	Strain Gages	Two (wired in compression bridge)	Tube Supports (Figure 24)
13 14 15 16	Strain Gages	Two (wired in bending bridge)	Support Angle, Right Side, between Shield and Stub Sill (Figure 10)
17 18 19 20	Strain Gages	Two (wired in bending bridge)	Support Angle, Left Side, between Side Sill and Shield (Figure 11)
21 22 23 24	Strain Gages	Two (wired in bending bridge)	Support Angle, Left Side, between Shield and Stub Sill (Figure 11)
26	Accelerometer	N.A.	Stub Sill (Figures 23,24)
27 28	Strain Gages	Four (wired in four active arm bridge)	Side Frame (Figure 25)
29 30	Strain Gages	Four (wired in four active arm bridge)	Side Bearings (Figure 26)
31	Wheel Revolution Counter	N.A.	Wheels
32	Time Code Recorder	N.A.	N.A.

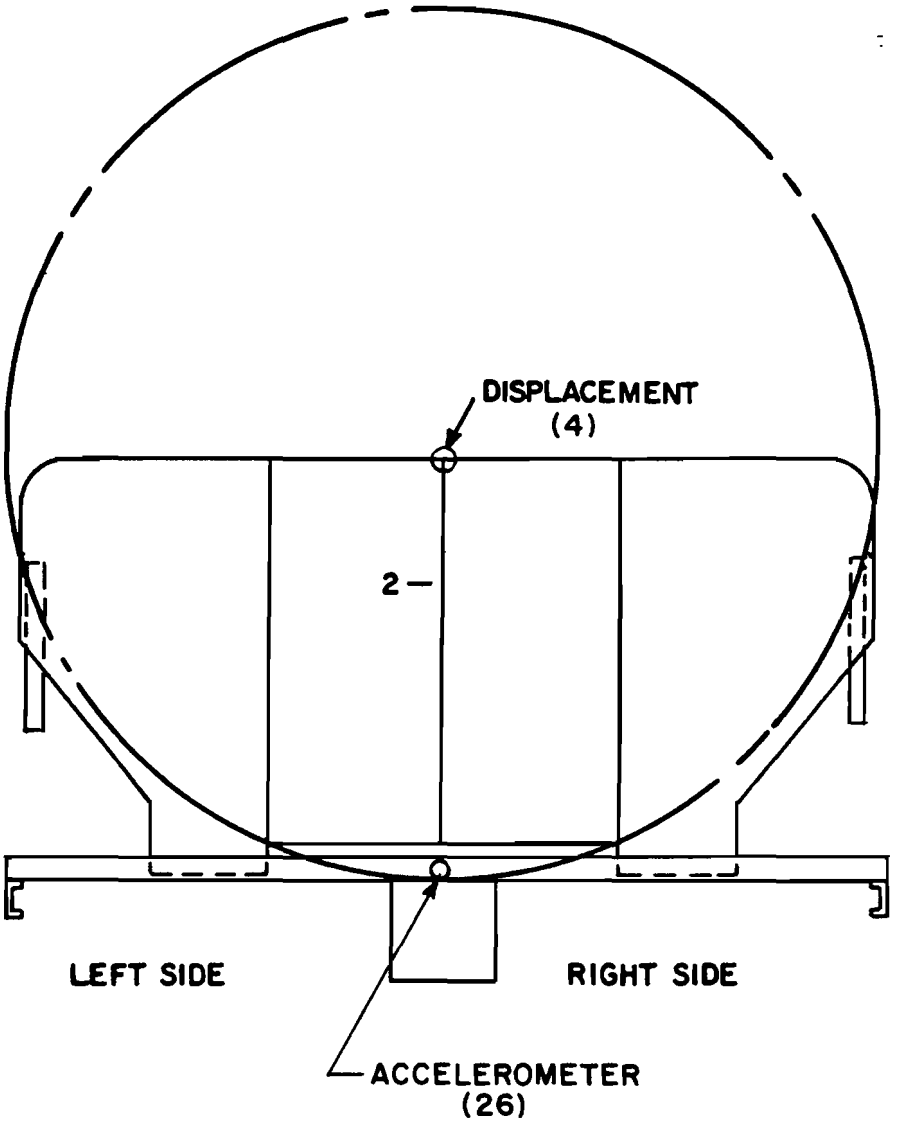

FIGURE 23. GAGE PLACEMENT ON FRONT OF SHIELD. Gages front and back at position 2 wired as bending bridges.

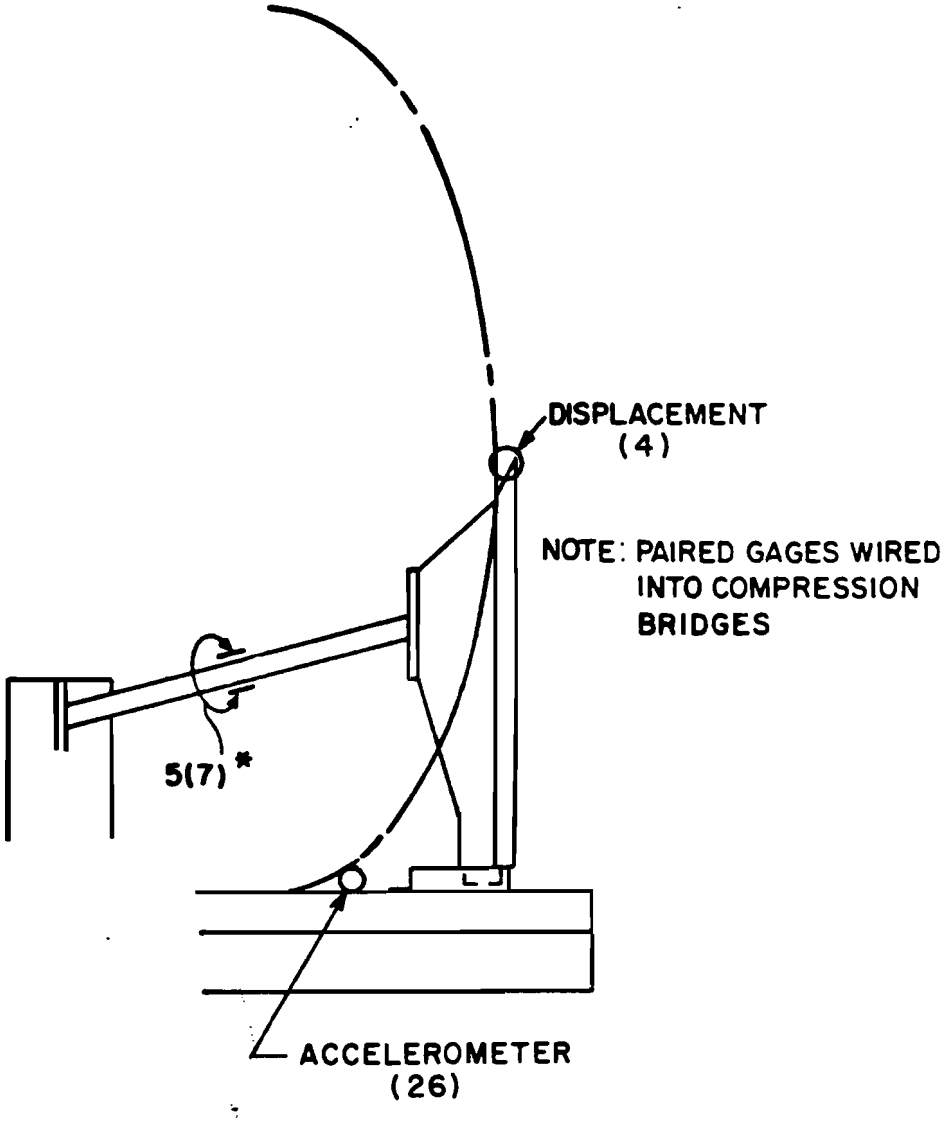

FIGURE 24. GAGE LOCATIONS ON TUBE SUPPORTS.
*View shown is for left side of car, right side gage channel is Number 7.

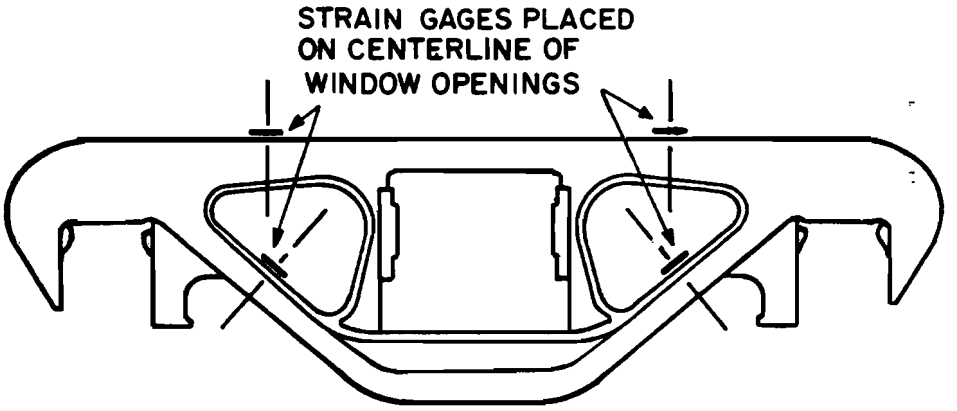

FIGURE 25. PLACEMENT OF SIDE FRAME STRAIN GAGES. Gages on each side frame are wired into a four active arm bridge; Channel 27 right side frame, Channel 28 left side frame.

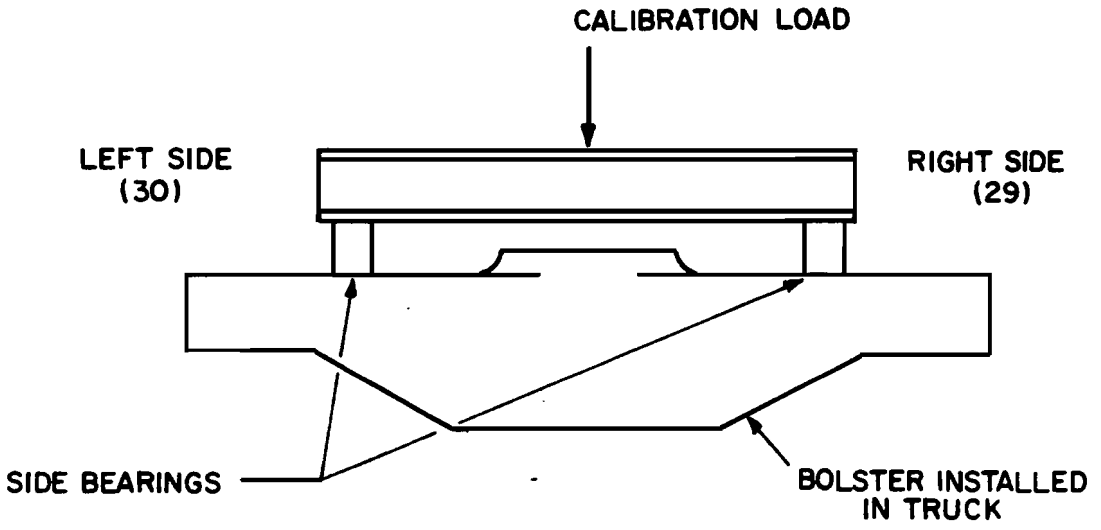

FIGURE 26. SIDE BEARING LOAD CELLS AND CALIBRATION LOAD PROCEDURE.

TABLE 6.—GAGE ALLOCATIONS TO RECORDERS

Recorder 1		Recorder 2	
Gage Channel	Type of Transducer	Gage Channel	Type of Transducer
2	Strain Gage	2	Strain Gage
4	Displacement		
5 7	Strain Gages (Tube Supports)		
13 14 15 16	Strain Gages (Support Angle)		
		17 18 19 20	Strain Gages (Support Angle)
		21 22 23 24	Strain Gages (Support Angle)
		26	Accelerometer
27 28	Strain Gages (Side Frame)	27 28	Strain Gages (Side Frame)
29 30	Strain Gages (Side Bearings)		
31	Velocity	31	Velocity
32	Time Code	32	Time Code

5. RESULTS - OVER-THE-ROAD TESTS

The over-the-road tests were conducted during September 1975. The first round trip was completed September 24-25th. The tank car was empty for this run. Speeds up to approximately 50 mph were obtained. There were no apparent significant vibrations of the shield or its supporting structure.

On the second trip the car was loaded with water to the maximum allowable 263,000 lb at the rail. The test run began Friday, September 26, 1975. Data were recorded to Kankakee, Illinois where the failure of the propane engine-generator set prevented recording data for the remainder of the trip to Champaign, Illinois. The return trip was conducted Tuesday September 30, 1975. Speeds over 50 mph were sustained for a long enough period of time to demonstrate that the car was susceptible to severe bounce motions in this speed range. There were numerous times when the main suspension springs went solid, which tended to excite low levels of shield vibration.

5.1 Data Analysis

After the tests, selected samples of the data from each channel were played back and displayed on an oscillographic record. Particular emphasis was given to examination of the data during times when severe vibrations of the car occurred. This review indicated that on many of the channels the signal levels were low enough to indicate a negligible response of the shield and its supporting structure. This is demonstrated by the data presented in Table 7, where the maximum ranges of the signal levels are presented for each of the channels. Note that all of the strain gage bridges, represent the output of two gages wired in a bending bridge so that the maximum strain on each gage of the bridge is approximately one-half the value shown.

TABLE 7.—MAXIMUM RANGE OF DATA SIGNALS ON OVER-THE-ROAD TESTS

Gage Channel Number	Type	Empty Car Run	Loaded Car Run
2	Shield Strain	± 90μ in./in.	± 200μ in./in.
4	Displacement	± .4 in.	± .5 in.
5	Side Support Strain	± 30μ in./in.	± 90μ in./in.
7	Side Support Strain	± 150μ in./in.	± 60μ in./in.
13	Support Angle Strain	± 300μ in./in.	± 200μ in./in.
14	Support Angle Strain	± 300μ in./in.	± 200μ in./in.
15	Support Angle Strain	± 300 in./in.	+ 1,000 - 600μ in./in.
16	Support Angle Strain	± 500μ in./in.	± 500μ in./in.
17	Support Angle Strain	± 700μ in./in.	± 100μ in./in.
18	Support Angle Strain	± 500μ in./in.	± 100μ in./in.
19	Support Angle Strain	± 1,600μ in./in.	± 500μ in./in.
20	Support Angle Strain	± 200μ in./in.	± 600μ in./in.
21	Support Angle Strain	± 300μ in./in.	± 700μ in./in.
22	Support Angle Strain	± 800μ in./in.	± 700μ in./in.
23	Support Angle Strain	± 1,600μ in./in.	+ 1,500 - 600μ in./in.
24	Support Angle Strain	± 1,000μ in./in.	± 600μ in./in.
27	Side Frame Load*	20,000 lb	130,000 lb
28	Side Frame Load*	30,000 lb	140,000 lb
29	Side Bearing Load	30,000 lb	90,000 lb
30	Side Bearing Load	35,000 lb	110,000 lb

*Above mean level.

Because of the low signal levels from the strain gage bridges these data were not processed any further except for the gages at the most highly stressed region on the angle, the location adjacent to the stub sill. The emphasis was given to analyzing and evaluating the side frame load data (Gage Channels 27 and 28), and the side bearing load data (Gage Channels 29 and 30). These analyses are described in the following sections.

5.2 Frequency Analysis

Selected data samples from over-the-road tests were analyzed to determine their spectral content. Samples of the vertical load data provided by the side frame strain gages, the strain data from the angles supporting the head shield, and the vertical accelerations measured by an accelerometer mounted on the stub sill were included in these analyses. A spectral analysis shows the dominant frequencies in the vibrational response of the structure and aids in establishing the frequency range to consider when sampling data for further digital processing. The results are displayed in plots of power spectral density.

5.2.1 Loaded Car Data—Figures 27 through 29 show data from the loaded car run at the region (approximately 50 mph) where the maximum response motions of the car were developed. Three frequency ranges are used to display this information. Figures 27a, b, and c, show the vertical truck load data. Note the presence of two major low frequency peaks, the first at approximately 2.5 Hz which represents car bounce motions, and the second at approximately 3.6 Hz which probably represents a pitching motion of the car. The cause of the narrow peak at 0.4 Hz is not known. Figure 27b shows the rapid decay in the vibrational level above approximately 5 Hz, the level being down about four orders of magnitude by 20 Hz. There is a slight increase in vibrational level in the 30 to 70 Hz range and again in the 200 to 450 Hz range with a local peak occurring at approximately 275 Hz. Vibrations in this range have been noted in similar data from other tests and probably represent the natural frequencies of the truck components themselves.

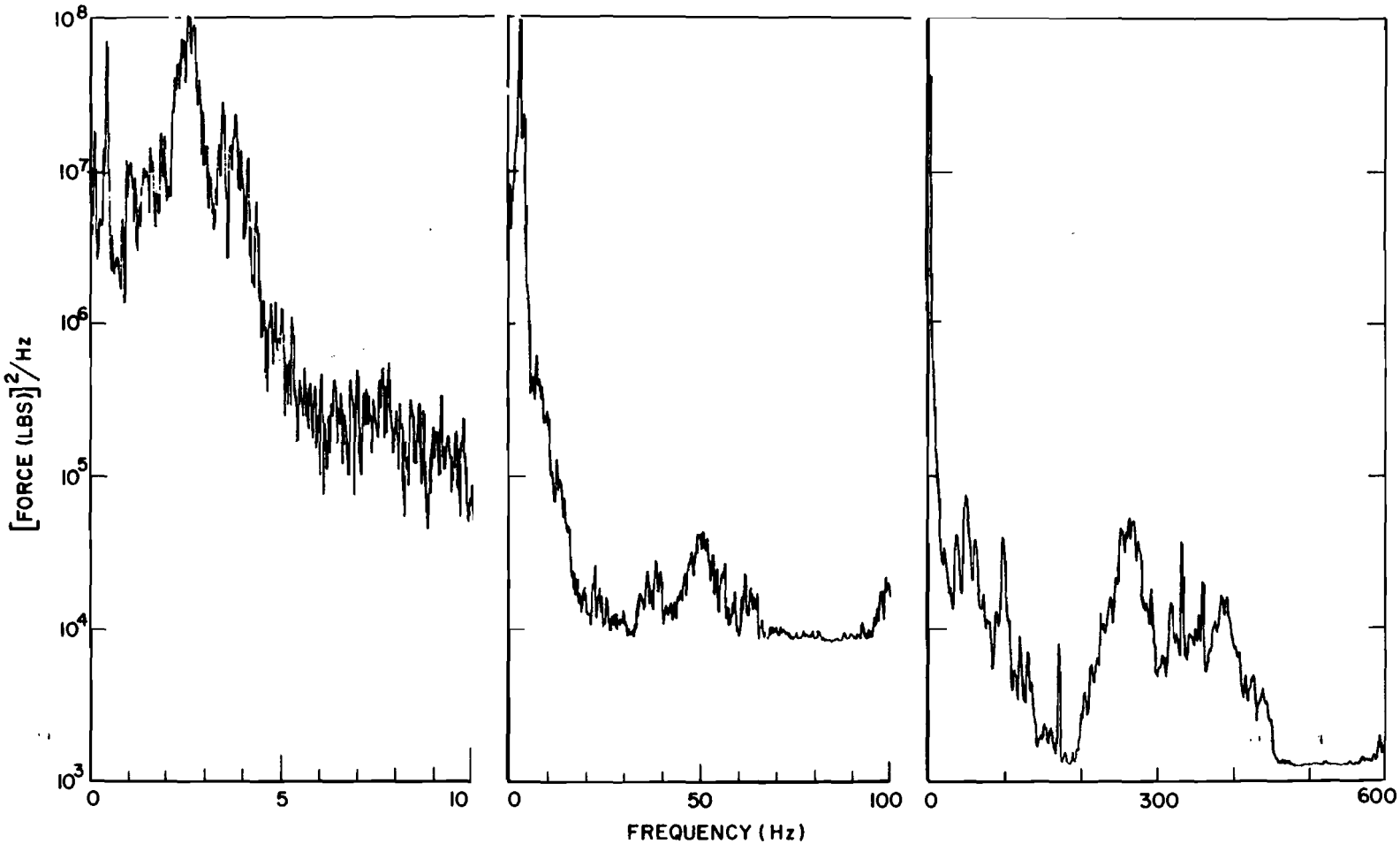

FIGURE 27. FREQUENCY ANALYSIS OF VERTICAL SIDE FRAME FORCE, LOADED CAR RUN.

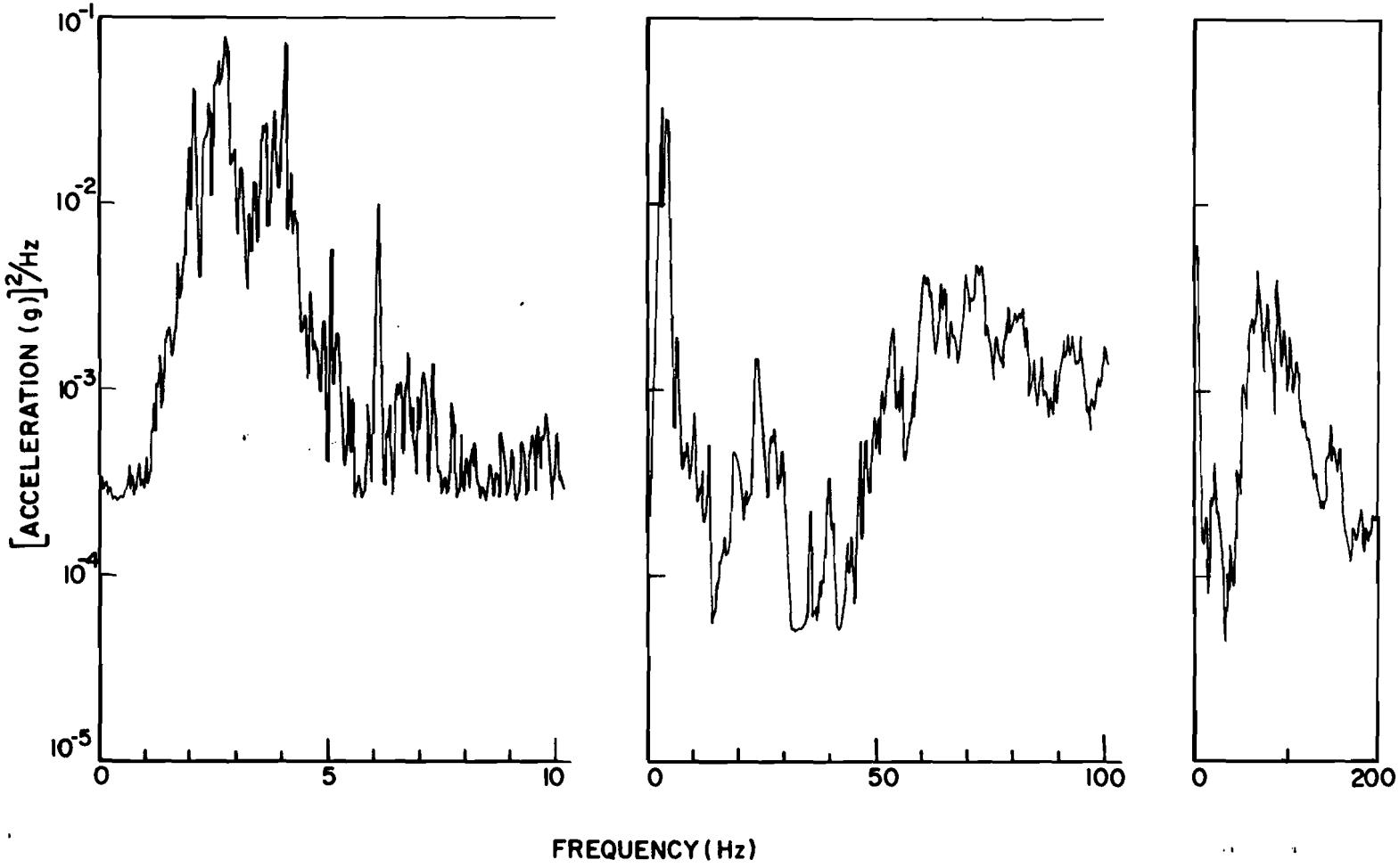

FIGURE 28. FREQUENCY ANALYSIS OF VERTICAL STUB-SILL ACCELERATION, LOADED CAR RUN.

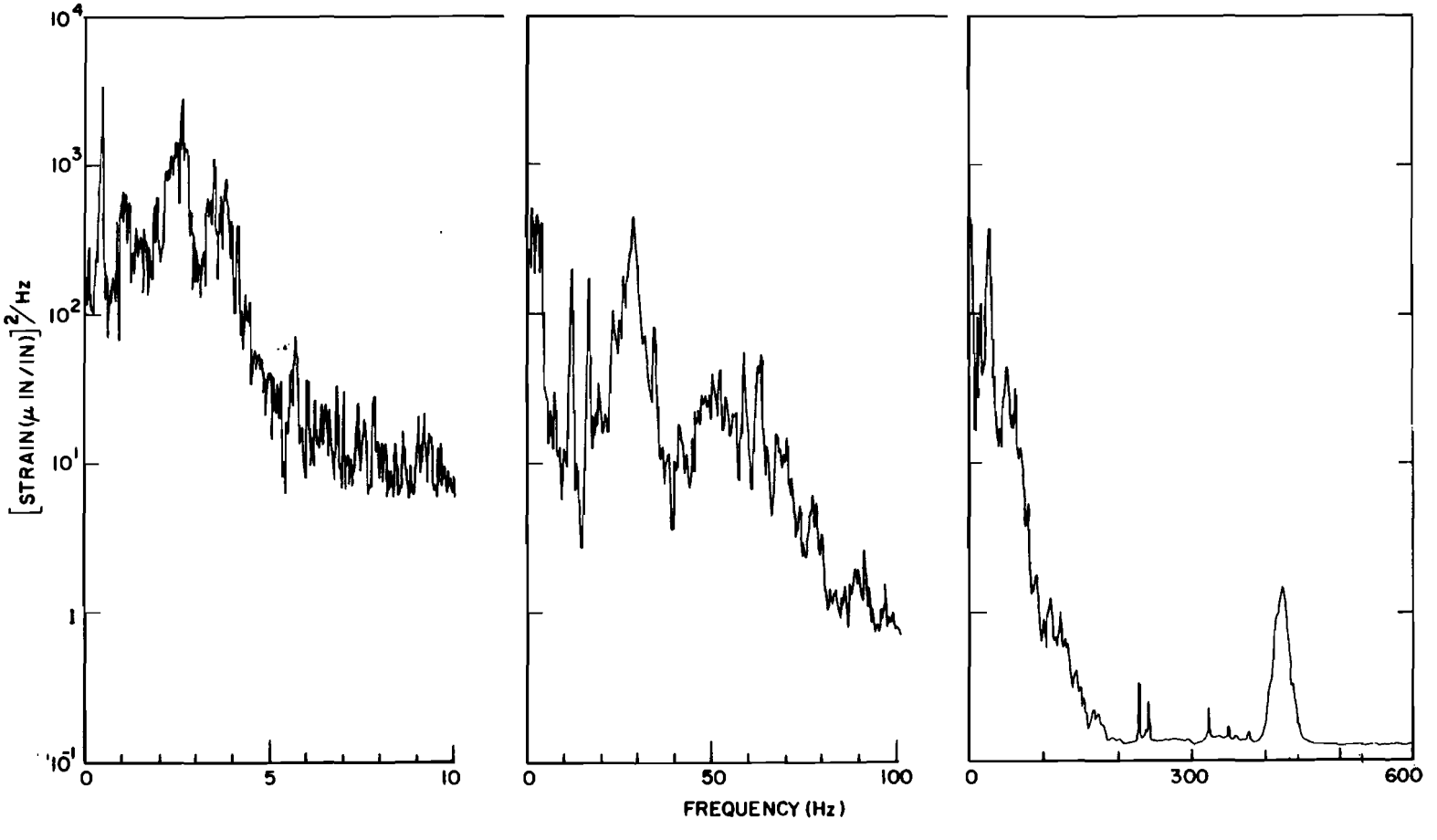

FIGURE 29. FREQUENCY ANALYSIS OF HEAD SHIELD SUPPORT ANGLE STRAIN, LOADED CAR RUN.

Figures 28a, b, and c, show results of the analysis of data from a vertically oriented accelerometer mounted on the stub sill. The low frequency data, Figure 28a, show the dominance of the low frequency 2.5 and 3.6 Hz car body bounce and pitch motions. Figures 28b and 28c show the presence of a band of local vibrational energy from approximately 50 to 150 Hz. The source of these motions is not known. The natural frequency of the accelerometer used for these measurements was 400 Hz which limited the useful accelerometer data to approximately 200 Hz.

Figures 29a, b, and c, show results of the analysis of data from the strain gage bridge on the horizontal angle supporting the weight of the head shield. The data were taken from Gage Channel 23 located adjacent to the stub sill on the vertical leg of the angle. This position was subjected to the most severe strains. Figure 29a shows the effects of the low frequency 2.5 and 3.6 Hz car body bounce and pitch motions. Figure 29b shows the presence of a broad band of vibrational energy in the 20 to 35 Hz region which peaks at 29 Hz. This vibration is clearly visible on time-history traces of the gage channel output and its role in establishing peak strain magnitude is apparent. It probably represents the natural frequency of the head shield vibrating vertically on the support angle. Figure 29c shows the rapid decay in vibrational strain about 50 Hz. It also shows the presence of a lower amplitude peak from unknown causes about 420 Hz.

5.2.2 Unloaded Car Data—Figures 30 to 32 show data from the unloaded car run. The data were obtained at speeds of approximately 50 mph, the maximum velocity obtained on the test. Figures 30a, b, and c, show vertical truck load data. Note that the dominant frequency is approximately 0.9 Hz in comparison to the 2.5 Hz frequency with the loaded car. Note also the lower level in the intensity of the vibration. The plot of the highest frequency range, Figure 30c, shows that the subsidiary peak at 250 Hz is still present.

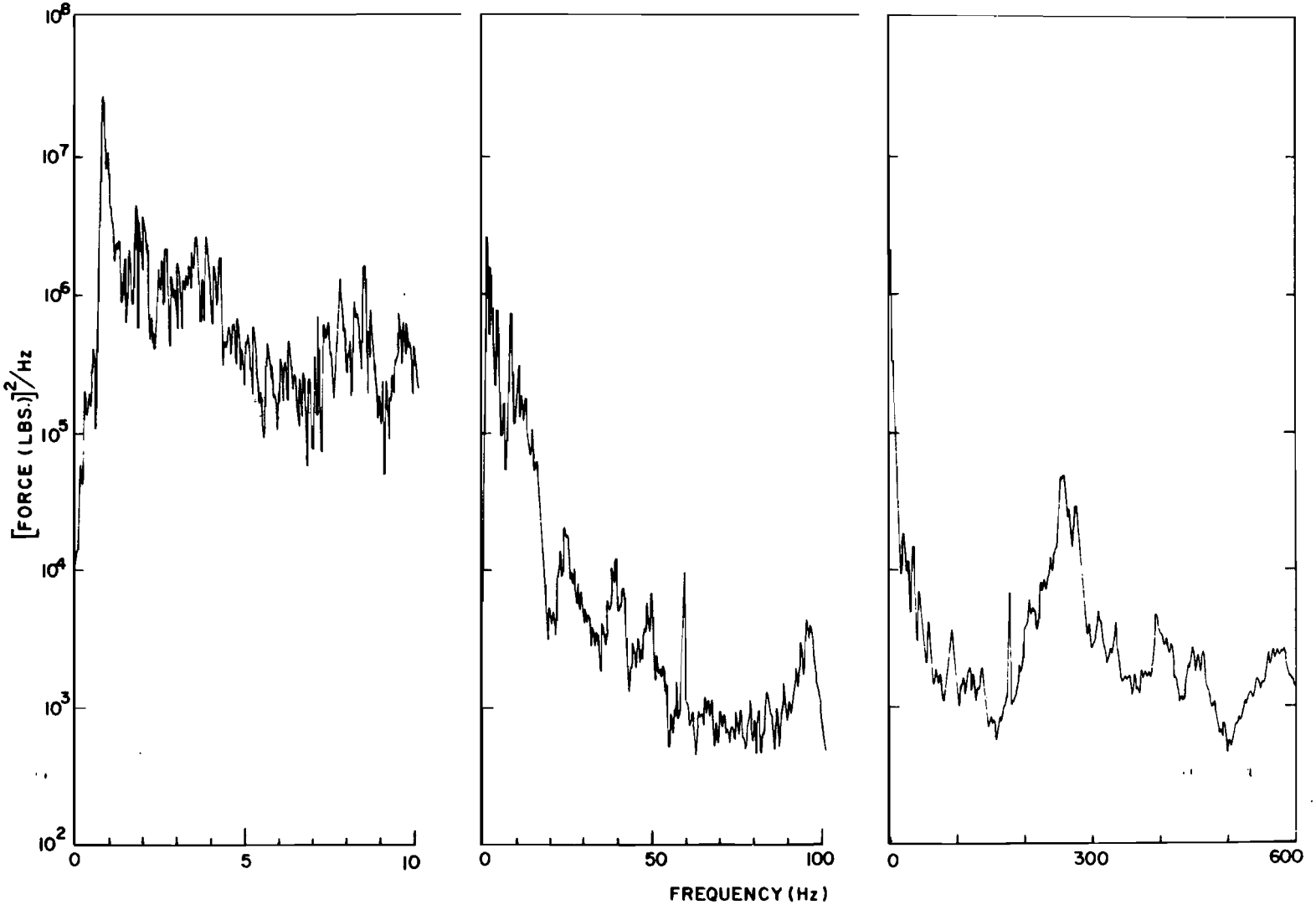

FIGURE 30. FREQUENCY ANALYSIS OF VERTICAL SIDE FRAME FORCE, UNLOADED CAR RUN.

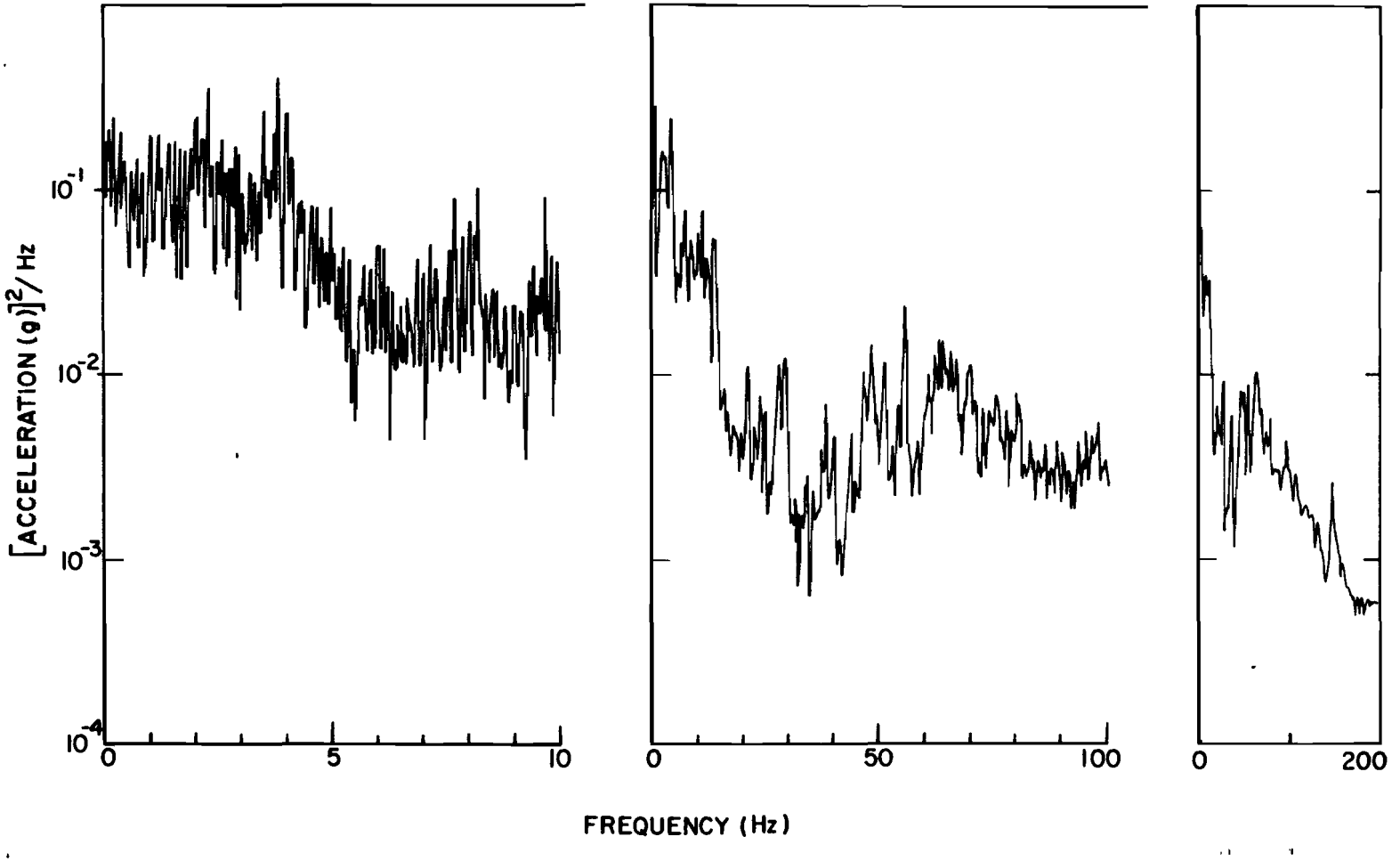

FIGURE 31. FREQUENCY ANALYSIS OF VERTICAL STUB-SILL ACCELERATION, UNLOADED CAR RUN.

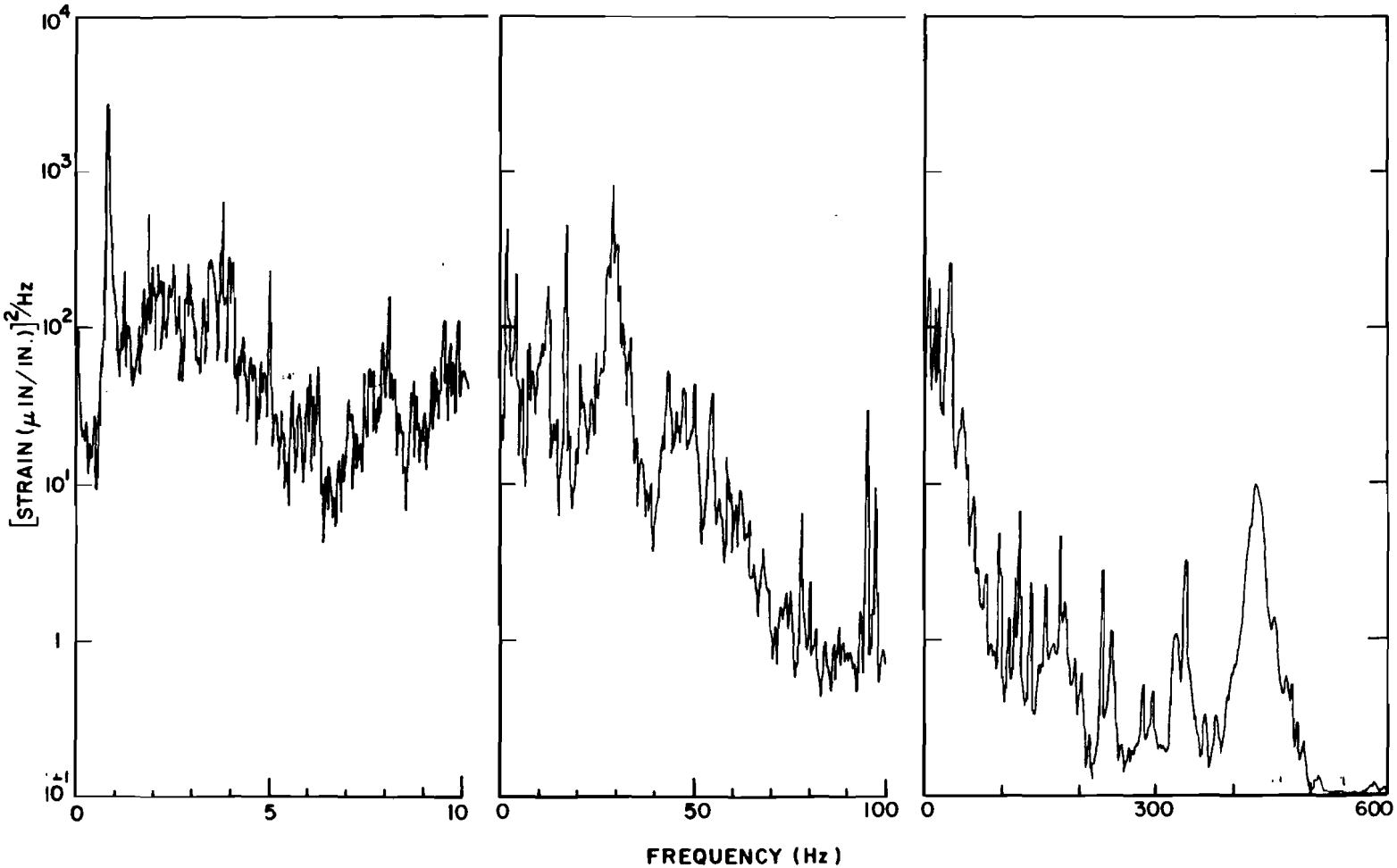

FIGURE 32. FREQUENCY ANALYSIS OF HEAD SHIELD SUPPORT ANGLE STRAIN, UNLOADED CAR RUN.

Figures 31a, b, and c, show results from the analysis of data from the accelerometers mounted on the stub sill. The maximum response is in the low frequency regime, below 5 Hz. Figure 31a shows the broad band characteristics of these data in contrast to the distinct frequencies shown in Figure 28a. Figure 31b shows the middle frequency range zero to 100 Hz. Note that the level of the vibrational energy is higher with the empty car than with the loaded car. The increase in the car body acceleration associated with the empty cars is also noted in the plot of the highest frequency range, Figure 31c.

Figures 32a, b, and c, show results from the analysis of data from the strain gage bridges, Gage Channel 23, on the horizontal angle. The dominant low frequency 0.9 Hz, is identified with the maximum load on the car (Figure 30a). Note the strong signal level peaking at 29 Hz shown in Figure 32b, which correlates with the loaded car data and is about the same amplitude level (Figure 29b). The presence of a broad lower amplitude vibrational level centered at 420 Hz is seen in Figure 32c. Again this is similar to what is observed with the loaded car data.

5.3 Truck Load Data

Data from the instrumented side frames were used to determine the vertical forces acting through the truck on the car. These data were processed by filtering the analog data at 50 Hz and digitizing it at 125 samples/second. The resulting digital record was then analyzed to determine the number of cycles in various load ranges. The intensity of the load environment under different speed conditions was also compared.

The fluctuating load data were summarized by a count of the peak loads between crossings of the mean level. This counting procedure provides an accurate summary of the load environment and permits convenient graphical comparison of various data sets. The data are presented on a load spectrum which is a plot of the peak levels (both positive and negative) of the alternating component of the load versus the number of times the load level is

exceeded in a given counting interval. A spectrum is developed by counting the number of times the load exceeds given incremental values from the mean static load over a given segment of data. Both positive and negative (if applicable) peaks are counted and the total counts at each level are reduced to a per mile basis for presentation.

Data from the instrumented side frames showed the the vertical force load environment was most severe when the car was loaded with water to the maximum rail load capacity (263,000 lb). The trucks on the test car (RAX 203) were equipped with D-3, 2-1/2 inch travel springs, which is a somewhat stiffer suspension than the 3-11/16 inch spring travel used in most current freight car trucks. Data from the tests show a severe load environment at speeds above 45 mph. At these speeds severe bounce load oscillations developed and there were many indications of the springs going solid, which resulted in high peak dynamic loads. Figure 33 shows load spectra for the vertical side frame force data. The data are segregated into three speed ranges, 15 to 30, 30 to 45, and 45 to 60 mph, to show the effect of speed on the intensity of these spectra. These results are based on the analysis of 39 miles of data in the 15 to 30 mph speed range, 58 miles in the 30 to 45 mph range and 17 miles in the 45 to 60 mph range. For comparison, empty car data are shown in the figure for the 45 to 60 mph speed range. For convenience the empty car data are plotted with reference to the nominal loaded car static load although in actuality the static load would be much less for this case.

Figure 34 shows similar load spectra for the truck bounce load. (This is defined as the instantaneous sum of the two side frame loads.) These data show the effect of the high dynamic loads associated with the suspension springs going solid when operating in the 45 to 60 mph speed range. The vertical load data measured on this test is much more severe than the data which have been measured on earlier studies of 100 ton capacity cars (Ref. 5). Load spectra for the side bearing loads are

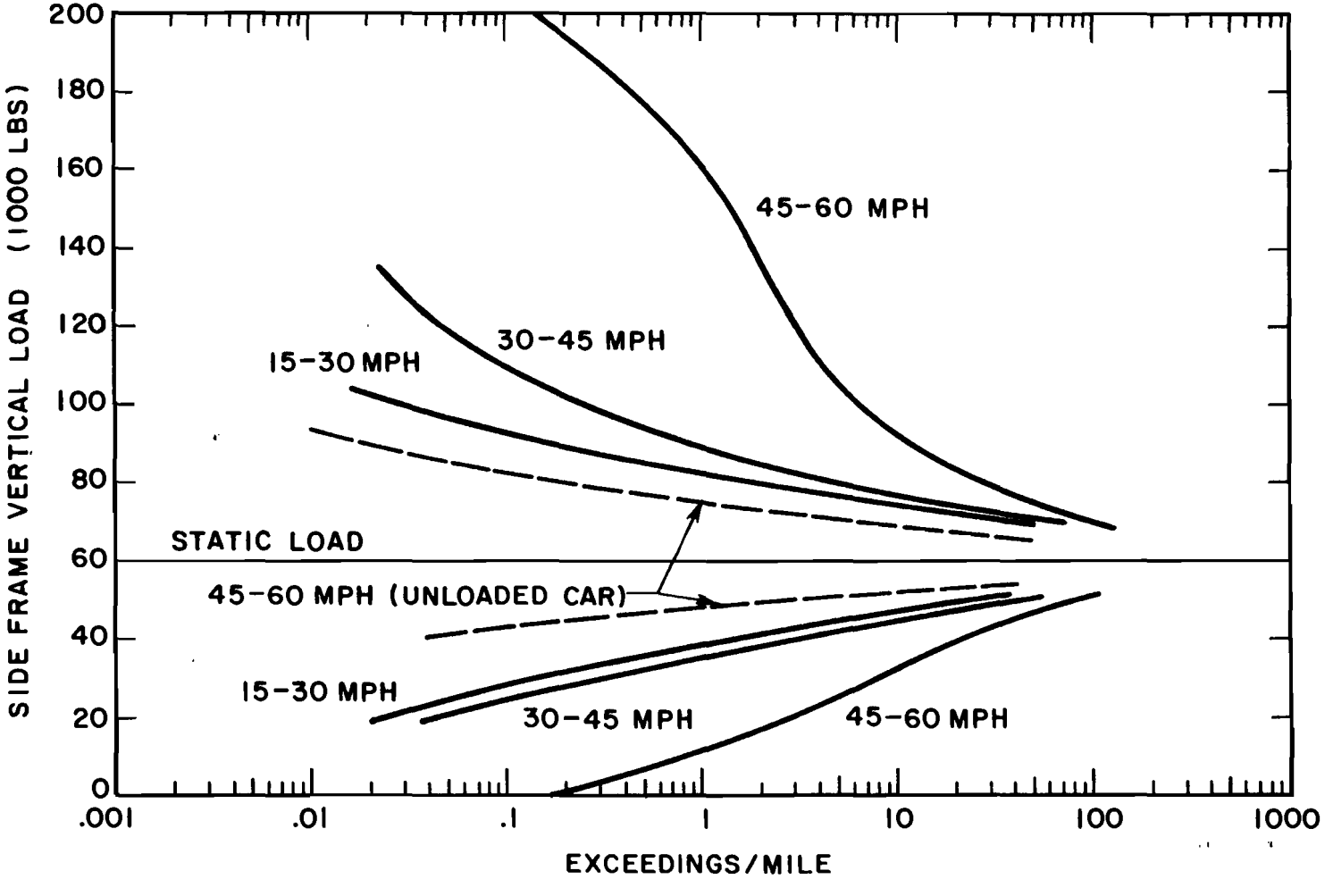

FIGURE 33. SIDE FRAME VERTICAL LOAD SPECTRA, LOADED CAR DATA EXCEPT WHERE NOTED.

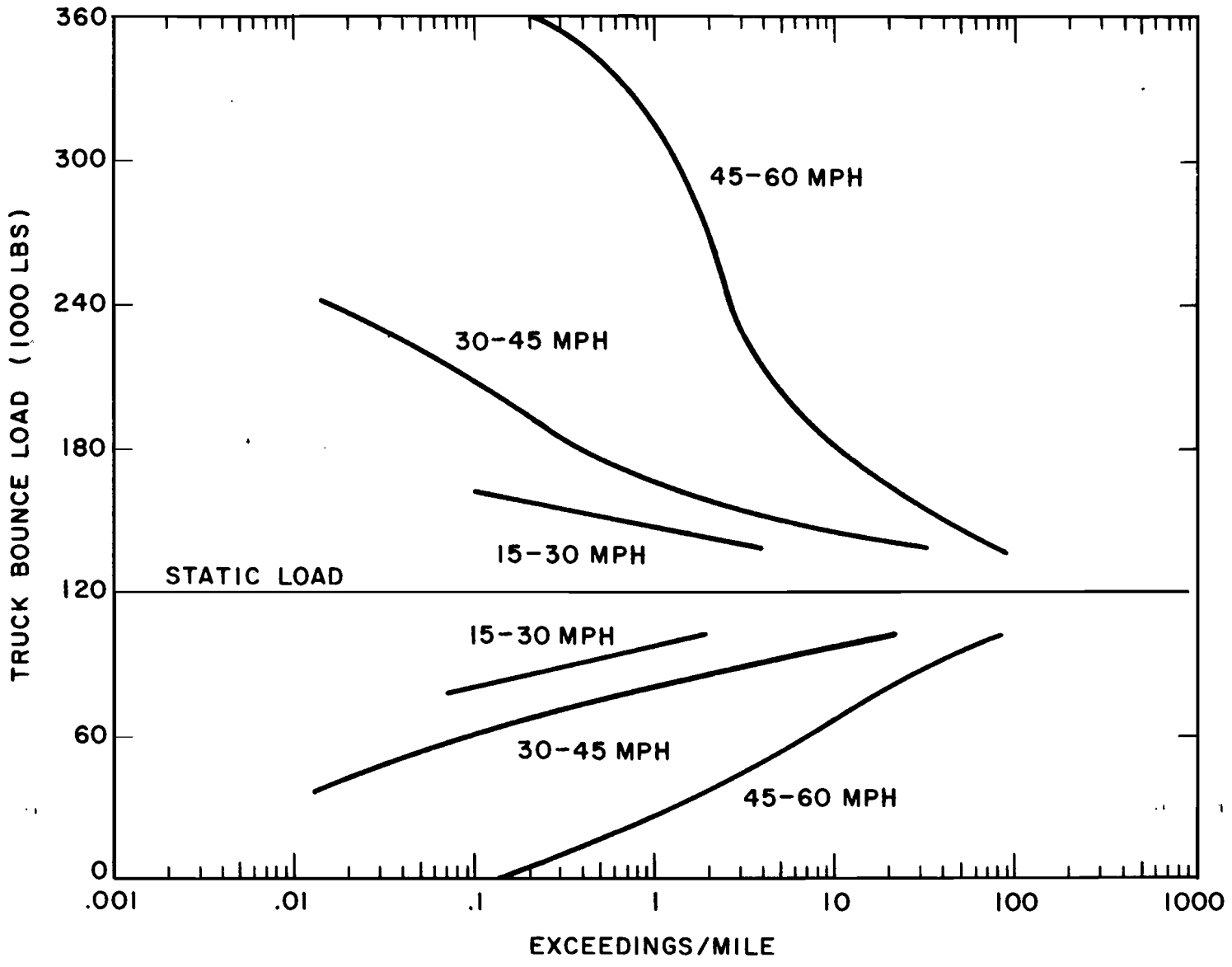

FIGURE 34. TRUCK BOUNCE LOAD SPECTRA, LOADED CAR DATA.

shown in Figure 35. The data which are plotted are the average for side bearing loads on the right and left sides of the car. Empty car data are also shown on the figure for the highest speed range.

5.4 Support Angle Strain Data

The strain data obtained from Gage Channels 23 and 24 on the support angle were analyzed in a similar way to the side frame force data, to determine the ranges and rates of occurrence of the fluctuating strains at the most highly strained position on the angle. The frequency analysis had indicated that the major frequency of excitation was approximately 29 Hz. Consequently in order to include these data and some of the higher harmonics, the signal was digitized at 250 samples per second.

A segment of data representing 8 miles of operation of the loaded car at speeds of approximately 50 mph, where there were numerous instances of the primary suspension springs going solid, was selected for analysis. This represented the most severe car body vibrations measured on the tests. The signals from the two angle strain gage channels adjacent to the left side of the stub sill were processed to give the strain at the top of the vertical leg, the most highly stressed position. A load spectrum of these data is presented in Figure 36. Note that the strains are well below the level where fatigue damage would be anticipated (1300 μ inch/inch). Thus it can be concluded that the over-the-road environment does not present a problem with respect to the accumulation of fatigue damage.

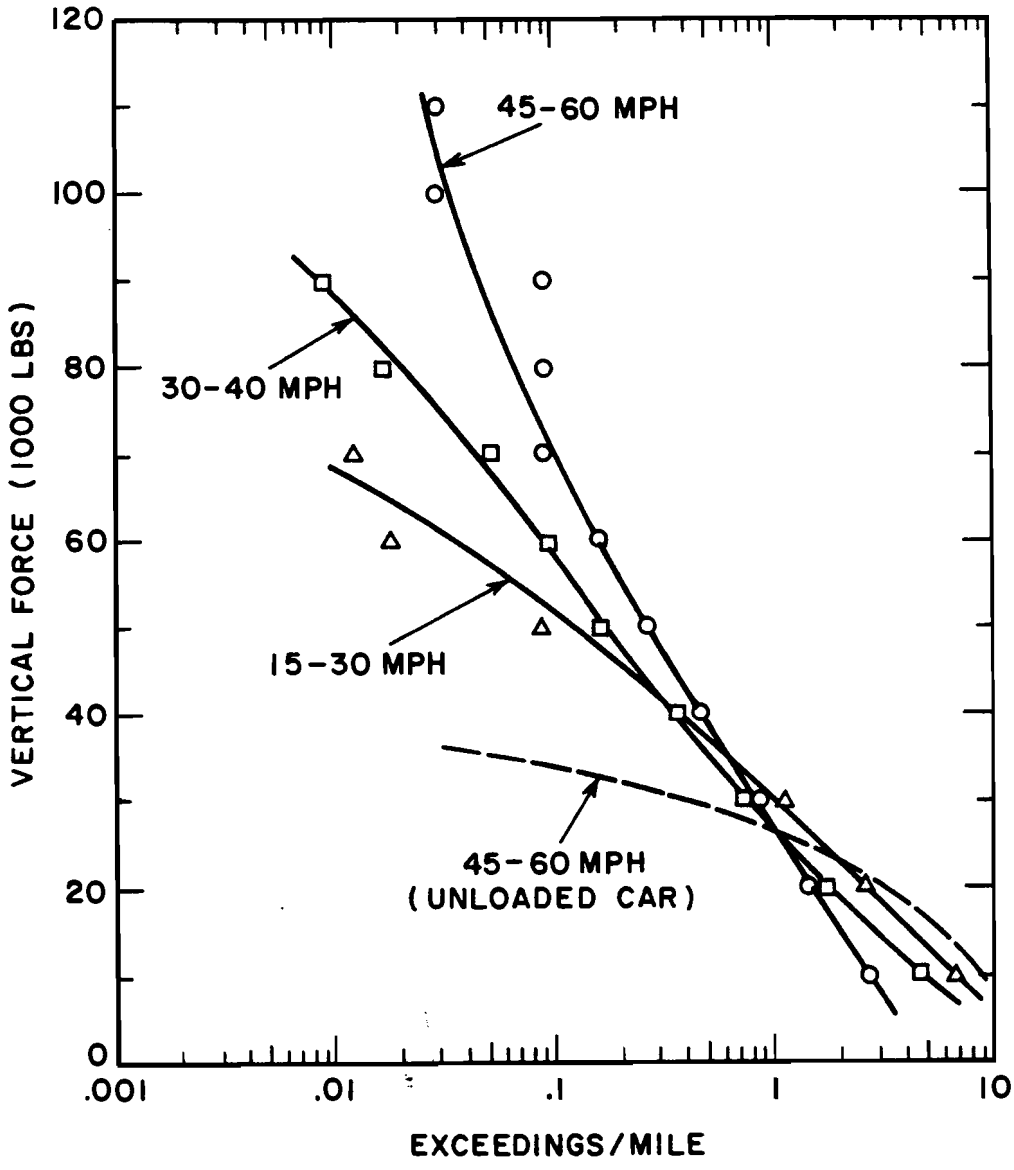

FIGURE 35. SIDE BEARING LOAD SPECTRA, LOADED CAR DATA EXCEPT WHERE NOTED.

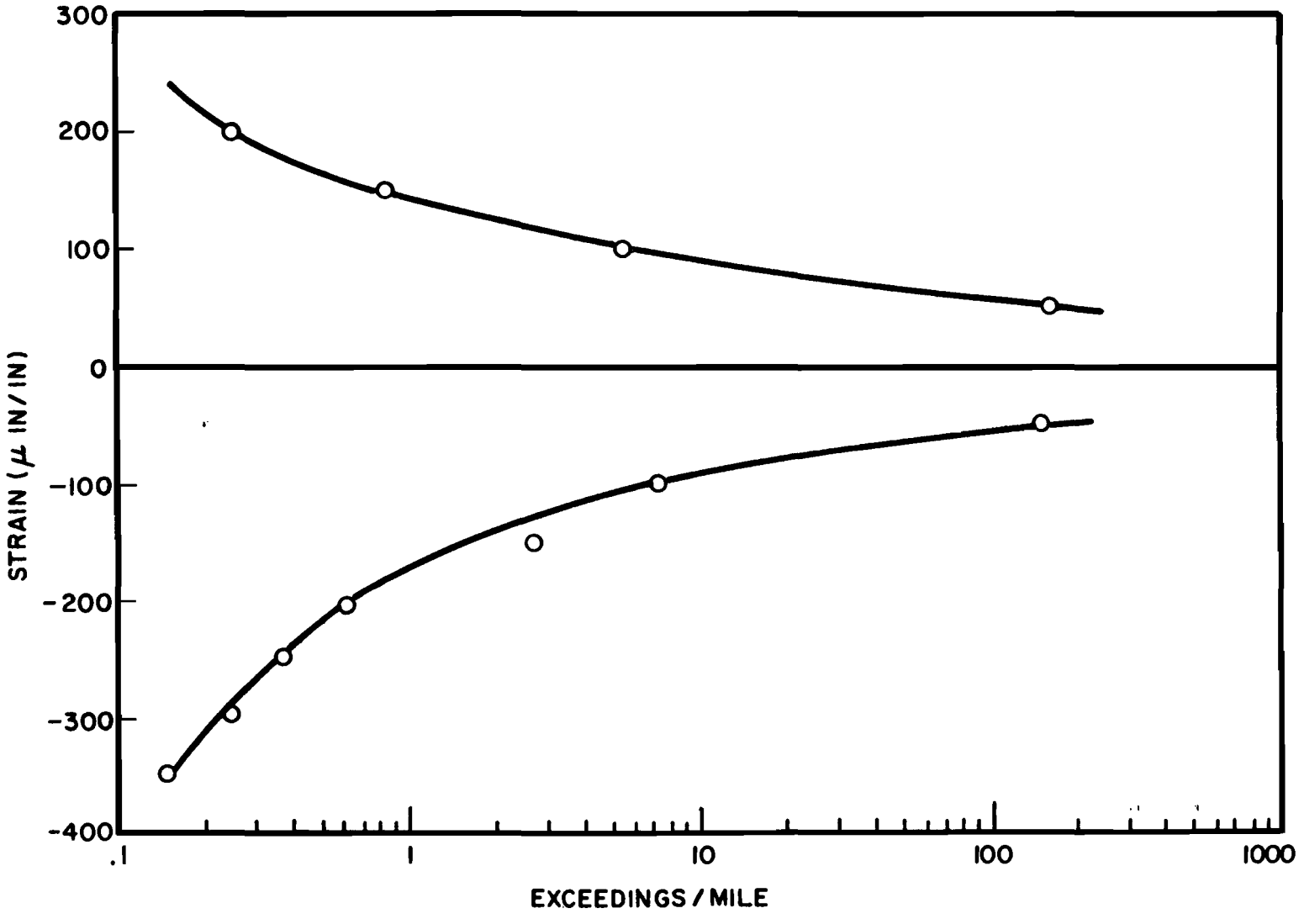

FIGURE 36. SPECTRUM OF STRAIN CYCLES, STRAIN ON UPPER ANGLE LEG AT STUB SILL, LOADED TANK CAR RUN.

6. GUIDELINES FOR HEAD SHIELD QUALIFICATION TESTING

The results from the test and analysis work conducted under this program can be used to suggest guidelines for future head shield qualification tests. These tests would be concerned with the resistance of the shield structure to fatigue damage, rather than the protection afforded to puncture of the shell.

Results from this project indicate that there are two basic factors which should be recognized when considering head shield qualification tests. These are:

- the fact that the car-coupling environment produces more significant effects on the shield and supporting structure than the over-the-road environment and,
- the fact that tests are necessary to demonstrate the shield performance because of the complex response of the shield to the dynamic service environment (whether it be car-coupling impacts or over-the-road)

The data which have been presented for the LTU head shield indicate that the car-coupling impact environment resulted in an expected finite fatigue life for the supporting structure of the shield at the most highly stressed location. An infinite life was projected for the over-the-road environment. These conclusions were also reached by the AAR/RPI study (Ref. 3). One would expect that the same relationship would hold for other head shield designs so that it would be sufficient to utilize the results from car-coupling impact tests alone for performing a qualification test.

One may wish to consider conducting a fatigue evaluation analytically by performing a dynamic analysis of the shield and car under simulated car-coupling impact conditions. The tests revealed, however, that it is desirable to obtain data through tests because of the complex dynamic response of the head shield and its supporting structure to the car-coupling impact environment. While dynamic analyses can provide insight into the parameters affecting response phenomena it may be impossible to obtain

an accurate quantitative description of dynamic response effects. In the tests it was noted that the response of higher-order vibrational modes gave significant contributions to the damage producing phenomena. These response phenomena will not be revealed by simplified analyses which account for only the fundamental vibrations of the shield structure. A complex structural analysis with an accurate dynamic representation of all structural characteristics would be required to predict motions and magnitudes of the loads like those which were measured. By testing in the actual physical environment the response parameters can be measured which have to be considered in the evaluation of the fatigue characteristics.

While the qualification test can be limited to car-coupling impact tests, one should recognize the strong dependence of the test results on the specific conditions under which the test is conducted. In this study, for example, the rate of accumulation of fatigue damage with the anvil car tests was eight times greater than with the hammer car tests. The reason for this difference is the fact that the higher modal frequencies of the shield supporting structure are significant in affecting maximum loads and stresses within the structure. Slight differences in properties of the acceleration phenomena associated with the placement of the shield on the test car and the condition of restraint and deceleration of the cars themselves, has an important effect in determining maximum stresses and strains within the structure. Therefore one should consider conducting at least two different types of car-coupling impact tests in the head shield qualification procedure so that there is a greater chance that the most significant dynamic phenomena will be obtained in the testing process.

In summary, the following guidelines are recommended for qualifying new head shield designs to resist accumulation of fatigue damage:

- the use of data from car-coupling impact tests to determine design adequacy
- the use of at least two different impact test procedures (e.g. hammer car or anvil car placement of shield, etc.) for gathering test data
- the utilization of sufficient instrumentation to determine stresses and strains at all critical locations in the shield and supporting structure
- conduct of tests over a range of impact speeds to at least 8 mph
- the projected life from the tests to be at least three times the anticipated service life of the car.

7. CONCLUSIONS

A prototype head shield for hazardous material tank cars was examined to determine the likelihood of fatigue damage developing under normal service conditions. Both car-coupling impact and over-the-road tests were conducted. The head shield withstood a total of 41 car-coupling impacts and 432 miles of over-the-road movement without developing apparent damage to the shield or its supporting structure.

Three different versions of the side supporting structure for the shield were included in the tests. The differences were in the flexibility of the side supports which connect the shield plate to the car bolster. As expected the shield with the most flexible side supports deflected most in response to the inertial loads associated with car impacts. For each design version the most severely stressed element was the horizontal support angle. This member spans between the two side sills and the stub sill and supports the weight of the shield. Within this element the highest stresses were developed at its junction with the stub sill. The stresses in this member were slightly lower with the more rigid side supports than with the flexible side supports.

The data obtained from transducers mounted on the structure were analyzed to determine the fatigue characteristics of the design. The analysis showed that car-coupling impacts produced an environment where finite life would be expected at the most highly stressed location in the supporting structure. The over-the-road operations revealed a less severe environment where fatigue damage would not be anticipated. The evaluation was based on the reported number of car coupling impacts that an average car would experience yearly and the velocity distribution of these impacts. A relatively small design change in the support structure for the shield would be sufficient to eliminate any possibility of fatigue damage.

The forces transmitted to the car body itself from the shield were determined for both the car-coupling impact and over-the-

road environments. These forces were transmitted through the side supports to the car bolster and through the horizontal supporting member to the side sills and stub sill. They were found to be of negligible magnitude on the over-the-road environment. The forces transmitted to the car during car-coupling impacts were significantly larger, but were still within the limits where they could be reacted by the existing car structure without causing damage. Thus the addition of the head shield to a hazardous material tank car is possible without altering the structural configuration of the end of the car.

Although the car structure basically has the capability of carrying the loads imposed by the shield, attention still must be given to the design details of the supporting structure of the shield. This study has revealed that there is the distinct possibility that fatigue damage can occur in these structural elements. The tests showed that severe environmental conditions, such as car coupling impacts, produced a complex response of the shield and supporting structure which excited many of the higher frequency modes of vibration and that the peak stresses were largely dependent on high frequency phenomena. Therefore attempts to model analytically the behavior of the shield to a severe operating environment must involve a sufficiently complex representation of the structure to adequately represent high frequency phenomena.

The complex response of the shield warrants the recommendation that the structural adequacy of a shield should be examined by performing tests under car-coupling impact conditions. Since the over-the-road environment was shown to have substantially less severe effects on the shield it need not be included in any verification tests of head shield resistance to fatigue damage. Because of the differences shown in the response of the shield to different car-coupling test conditions it is recommended that at least two types of car coupling impact tests be conducted during the performance tests, and it is further recommended that these include as a minimum, placement of the shield on the hammer car and anvil car.

REFERENCES

1. Johnson, M. R., "Evaluation of Prototype Head Shield for Hazardous Material Tank Car", Interim IITRI Report to TSC, May 1975.

2. "Specifications for Tank Cars", Association of American Railroads, Operations and Maintenance Division, Mechanical Division.

3. Phillips, E. A., "Phase 05 Report on Head Shield Fatigue Tests", RPI-AAR Tank Car Safety Research and Test Project Report RA-05-3-35, November 10, 1975.

4. Tetelman, A. S. and McEvily, A. J., Fracture of Structural Materials, John Wiley and Sons, Inc., 1967.

5. Johnson, M. R., "Analysis of Railroad Car Truck and Wheel Fatigue, Part 1, Service Load Data and Procedures for the Development of Fatigue Performance Criteria," Federal Railroad Administration Report FRA-OR&D-75-68, May 1975.

APPENDIX

REPORT OF INVENTIONS

The work conducted under this program resulted in the accumulation of significant data describing the car-coupling impact and over-the-road environments associated with railroad tank cars. In particular, the over-the-road data revealed conditions under which severe loadings of higher magnitude than heretofore reported can develop. These data were used to evaluate the fatigue characteristics of a prototype head shield.

After a diligent review of the work performed under this contract no new innovation, discovery, improvement or invention was made.

110 Copies